PLATED THROUGH RELIABILITY AND MATERIAL INTEGRITY RESULTS FOR 24 MATERIALS PROCESSED THROUGH LEAD FREE ASSEMBLY

Bill Birch, Jason Furlong
PWB Interconnect Solutions Inc.
Ottawa, ON, Canada
bill.birch@pwbcorp.com, Jason.furlong@pwbcorp.com.

ABSTRACT

The High Density Packaging Users Group (HDPUG) consortium have completed their 3rd phase investigation that combines plated through hole reliability and material integrity of printed wiring board test vehicles constructed with 24 different Pb-free capable materials. The selected materials in the study included four high Tg, filled FR4 materials, twelve high Tg halogen-free FR4 materials, and eight high speed materials. The study contained a total of 24 different constructions built by a single high-end Asia based PWB manufacturer. Materials testing were performed to determine there survivability through Pb-free reflow by measuring capacitance changes to determine levels of degradation within the B and C stage dielectric materials. The materials were also tested before and after reflow assembly using Interconnect Stress Testing (IST) methodology. The test vehicles combined both via reliability and materials analysis testing capabilities, using two specially designed IST coupons with via to via spacing of both 0.040" (1mm) and 0.032" (0.8mm), All products were constructed with 20 layers, laminated to an average thickness of 0.115" (2.92mm), and drilled with 0.010" (0.254mm) vias, producing an aspect ratio of 11.5 to 1. Twelve materials were investigated with two different glass styles and resin contents. The materials were base-lined as built and then compared after 6X Pb-free (260°C) reflow, the electrical results were compared to traditional microsection analysis to demonstrate the levels of correlation achieved. In addition, some materials were submitted into testing with the prior knowledge that material damage was present following the 6 cycles of assembly. Failure analysis was completed after IST thermal cycling testing and compared to the materials relative performance.

INTRODUCTION

Previous HDPUG consortium studies have identified significant challenges in complex multilayer applications with the printed wiring board (PWB) materials ability to survive multiple exposures through Pb-free assembly reflow [1, 2, 4, 5]. Specifically related to the confounding influence of quantifying the plated through hole (PTH) reliability in situations where material damage is known to be present [1]. One of the key influences previously noted was the effect of via to via spacing (grid) on the materials ability to survive through Pb-free assembly [1, 2, 4, 5].

The laminate industry has recently released new materials that they claim have improved survivability when exposed to multiple passes through a Pb-free assembly application. There was much interest in the consortium to evaluate these materials. This is the third study to quantify materials reliability, the same test vehicle (with minor modifications) has been used in each of the past studies. The latest revision of the Materials Reliability Test Vehicle (MRT-5) introduced minor changes to the previously reported revision "MRT-3" [3]. Changes included adding modified pad configurations for the pad pull test vehicle, used to measure for Hot Pin Pull, Cold Pull and Ball Shear testing of surface pads.

This paper reports the combined results of the IST thermal cycle testing and Materials integrity Testing using the DELAM methodology. In addition to this paper, there are three other supporting papers reported separately as part of the Pb-free Materials 3 Project. 1) Conductive Anodic Filament (CAF) Performance of PWB Materials Before and After Pb-free Reflow. 2) Lead-Free Laminate DMA and TMA Data to Develop Stress versus Temperature Relationship for Predicting Plated Hole Reliability. 3) Impact of Pb-free Assembly on Laminate Electrical Performance for High Layer Count High Reliability PCBs.

The goals for the various levels of testing were to:

- Characterize the performance of 12 recently released Pb-free compatible materials using the MRT-5 test vehicle.
  - Focusing on 20 layer constructions only, with 12 materials produced with both 58% and 69% resin content configurations.
  - Identify materials that are robust through Pb-free assembly reflow designed with 1mm/0,040" and 0.8mm/0.032" via to via spacing's.
  - Include new High Tg halogen free materials.
  - Include mid-level electrical performance FR4 and very high speed materials.
- For the FR4 and halogen free materials, focus on those that are expected to be more thermally robust and have better electrical performance characteristics while remaining cost effective materials.

- Evaluate the IST coupon design to determine if the DELAM methodology provides an effective non-destructive capability for understanding how to utilize capacitance measurements to confirm consistency of product construction, dielectric thickness and identify the presence of material damage both during and after Pb–free assembly.

MRT-5 Printed Circuit Board Design

The MRT-5 PWB test board used for this study is shown in figures 1, 2 and 3. The test board contains two IST coupons that are specifically designed to combine via reliability and material survivability testing. Both coupons contain a 0.25mm (0.010") drilled hole size, one coupon is located on a 1mm/0.040" grid and the other coupon has a 0.8mm/0.032" grid. The via chains on both grids in the IST designs are designed to be identical, both using the same hole size, including the use of non-functional pads on plane layers only, etc. Complete design details are reported separately [3].

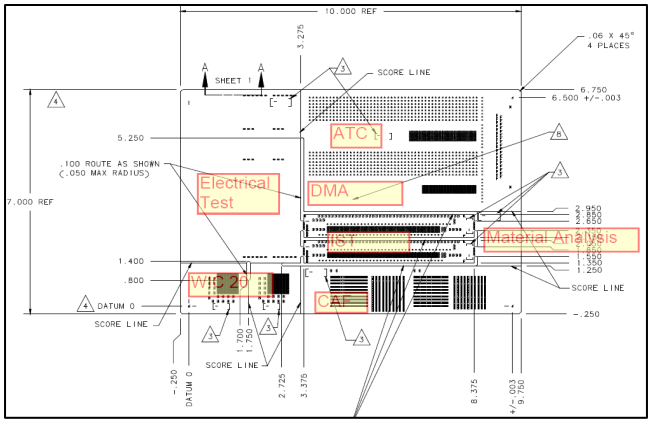

Figure 1: MRT 5 Test Board

The MRT-5 test board was stepped and repeated 4 times (2 by 2) onto a 610MM (24") x 457mm (18") production panel, see figure 2 for production panel lay-out. For this study a minimum quantity of 6 production panels were produced, resulting in a minimum of 24 coupons of each type. Subsequent testing was carried out on both non-stressed (As Built) and stressed (6x260°C Reflow); this effectively results in 12 coupons of each type for each test condition. For the purposes of increased statistical confidence a higher number (18+) is recommended, the lower quantity was determined by considering a compromise between statistical validity and containing the escalating costs associated to the cost of fabrication and all types and levels of testing.

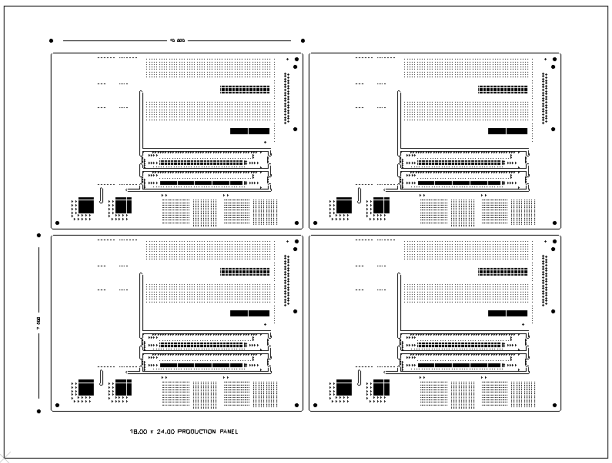

Figure 2: PWB Fabricator Production Panel

Following the production of the 24 different material types (at Viasystems in China) the production panels were pre-routed to enable easier removal (singulation) of certain coupon types and then profile routed into individual (10"/254mm x 7"/178mm) test boards. Figure 3 shows a pre-routed individual test board.

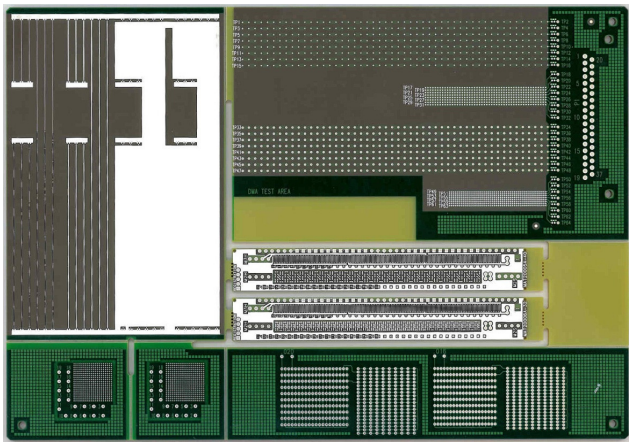

Figure 3: Picture of an actual MRT-5 test board

Material Stack-ups

Small labels with material codes were included near each dash number box for each coupon on the panel. This was done to ensure traceability back to the original panel once all the coupons were broken out of the panel following assembly. Two IST coupons are in each board design as shown in Figure 4. The IST design part numbers are MAT20006A-32 (0.8mm/0.032") and MAT20005A-40 (1mm/0.040") respectively. Note the design is generic and can be designed for any number of layers, copper weights and internal constructions.

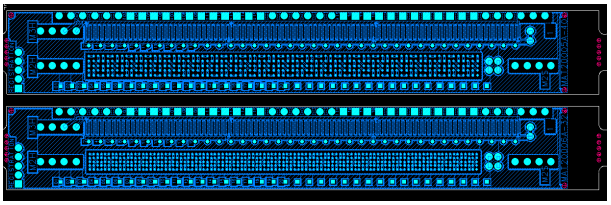

Figure 4: 0.8mm/.0.032" and 1mm/0.040" IST Coupons

Four different sets of IST coupons were tested for via reliability and Pb Free survivability; the 4 sets were comprised of two groups of 8 coupons with 0.8mm/0.032" grid and two groups 8 coupons with 1mm/0.040" grid. The first condition was "As built" (non-stressed) to establish a baseline reference. The second condition was after 6X 260°C reflow assembly cycles (stressed).

Product Construction

The "standard" 20 layer construction was designed with an overall resin content of 58%. Figure 5 shows the configuration of both B and C stage materials. The "high resin content" was constructed with an overall resin content of 69%. This represents very complex designs and worst case constructions that would typically have higher layer counts (such as 26 or 28 layers) in a similar thickness.

The 58% stack-up combined both a C stage using a 1 ply 2116 (53% resin) and a B stage using 2 plies of 1080 (62% resin), this should achieve a pressed thickness of 0.127mm/.005" and 0.137mm/.0054" respectively. See figure 5 for full 58% resin stack-up construction "A" details.

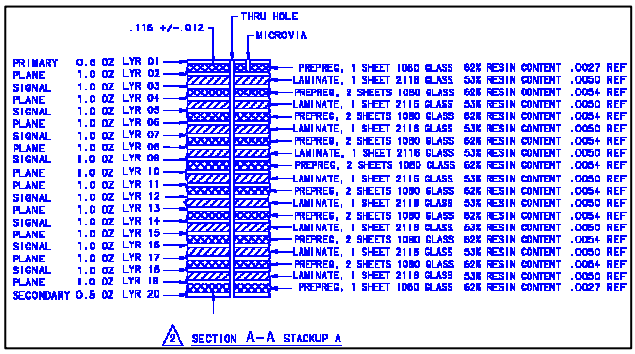

Figure 5: 20 layer stack-up "A", 58% resin

Note: Microvias were ablated from layer 1 to layer 2, this was required for interconnections used in the S-parameter impedance test board design.

The 69% stack-up combined C stage using 2 plies of 106 (71% resin) and B stage using 2 plies of 1080 (67% resin), this should have achieved a pressed thickness of 0.107mm/.0042" and 0.152mm/.006" respectively. See figure 6 for full 69% resin stack-up construction "B" details.

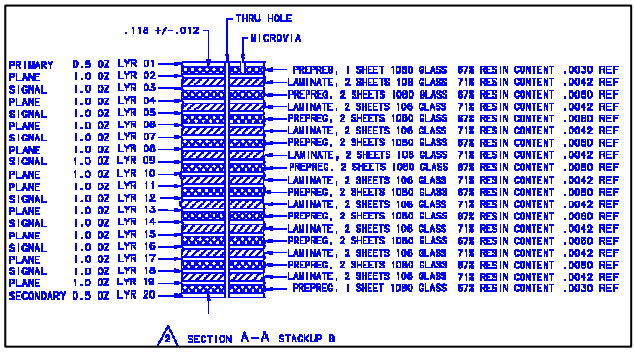

Figure 6: 20 layer high resin stack-up "B", 69% resin

Materials

The materials selected for this study were chosen from a large group of candidates, to keep the total to a manageable number, 12 materials, with 2 different constructions each, low and high resin constructions as shown in figures 5 and 6. Table 1 identifies all tested materials; a coding system was created and will be referenced throughout this report. HDPUG members have access to the cross-reference that identifies each specific materials tested in this study. The material coding using a single letter (E.g. A, B, etc.) is the 58% resin content construction. The material coding letter followed by a B, is the same material (resin system) but used the 69% resin content construction.

Table 1

EMPPS Coding	Stack-up	Resin Content %
High Tg FR4:		
A	A	58
AB	B	69
B	A	58
BB	B	69
Halogen Free FR4:		
C	A	58
CB	B	69
D	A	58
DB	B	69
E	A	58
EB	B	69
F	A	58
FB	B	69
G	A	58
GB	B	69
H	A	58
HB	B	69
High Speed FR4:		
I	A	58
IB	B	69
J	A	58
JB	B	69
K	A	58
KB	B	69
L	A	58
LB	B	69

PCB Surface Finish

The PCB finish chosen for this testing was immersion silver. The actual finish used was not critical, provided it remained solderable after 6X reflow at 260ºC and did not include a nickel under-layer, as a nickel under-layer could potentially affect many of the results.

Process Used to Simulate Pb Free Assembly

Celestica performed the six reflow cycles to simulate the affects of assembly and rework using a BTU Pyramax150N 10 zone forced convection oven. Figure 7 shows the thermal profile that the test boards received. Based on this thermal profiling with thermocouples the board reached a maximum temperature of 260°C. The logic used for specifying six total cycles is based on three thermal excursions being equivalent to an assembly cycle of two passes through an SMT oven and one localized soldering step. Two additional thermal excursions would simulate a BGA removal and replacement, and one additional for touch up. The six thermal excursions is a simulation of the complete assembly and rework process. All test boards were vacuum sealed by the PWB manufacturer; all passes through the oven were completed without a prebake.

Preconditioning Profile

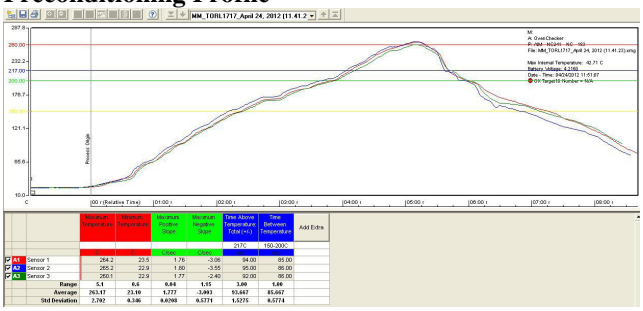

Figure 7: SMT Reflow Oven Thermal Profile

Table 2. Parameters used to create the reflow profile.

Profile Elements	*10 Zone Convection Oven Recommended*
Ramp Rate to 217°C Peak	Linear Ramp desired. Can have a small soak period. Usually 1 to 5°C/sec. No more than 2°C/sec
Pre-heat Temperature	Usually measured from 150°C to 200°C. Times within this temperature range are usually 60 to 120 seconds
TAL (Time above 217°C Liquidus)	Target 60 to 90 seconds
Time Within 5°C of Max Peak Temp.	10 to 20 seconds ok. Usually will be lower time.
Target Peak Temperature	**260°C Minimum +5°C / -0°C**
Ramp Down Rate	Target from 1.5°C/sec to 2.5°C/sec with normal oven cooling configuration
Reflow Atmosphere	Run all samples in air. (Worst case scenario)
Total Time in Oven	Usually 4 to 6 minutes
Thermocouples Attachment	Require minimum of 3 T/C's to properly profile raw card. (Leading Edge + Centre of Card +Trailing edge) are recommended locations.

Separate "scrap" cards were used to establish the reflow profile for each of the two (low & high resin content) configurations. A picture of where the thermocouples were attached to the profile card is shown in Figure 8.

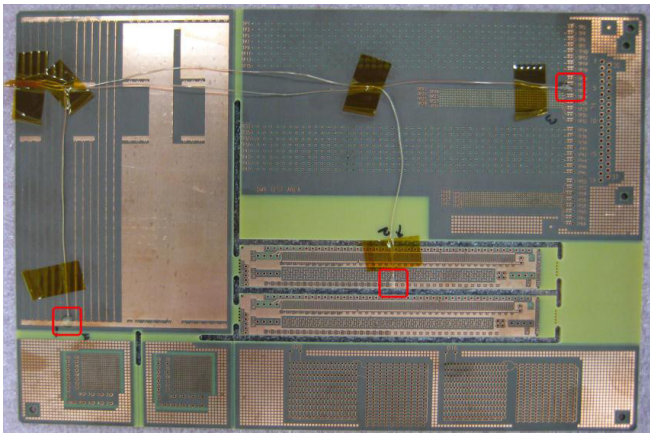

Figure 8. Reflow Oven Profile Board

Pre-conditioning Procedure

Boards were not baked prior to reflow. Panels were taken out of the packaging material and used as received. Prior to the start of the pre-conditioning run, the profile was verified again to validate that nothing had changed between when the profile was originally generated and when the actual boards pre-conditioning runs took place. During the actual runs, the cards were introduced into the oven to guarantee a minimum board spacing of at least 2 zones. This was to ensure that there were no thermal interactions between cards.

Additionally, each PWB was cooled to room temperature before being reflowed again, to guarantee that each card experienced the same thermal excursion between profile runs. After cooling, five 0.8mm/0.032" IST coupons from each material were re-measured on the DELAM tester. Small labels with the numbers "1 to n" were attached near each dash number box on each coupon on the panel. This was done to ensure traceability back the original panel once all the coupons were broken out of the panel at the end of the pre-conditioning. A tracking sheet was used to manually track and record all boards through the reflow process.

Prior to the start of the preconditioning, a photograph was taken of one panel from each dash number. After all subsequent reflow cycles the panels were inspected for any defects. All defects were recorded in the tracking sheets and photographed noting the defect locations, type and run number. After the completion of six reflow cycles, 1 panel from each dash number was photographed for comparison purposes to the incoming board condition.

Summary - Pre-conditioning Results at Celestica.

Most materials did not show any visual defects after reflow preconditioning. Three materials exhibited surface blistering (Materials D, DB, and EB) after 1 or 2X passes through the reflow oven.

DELAM Coupon Design and Protocol for Material's Survivability through the 6X 260 ° C Assembly Cycles

The laminate robustness methodology associated to the DELAM testing protocol utilizes a section of the IST coupon; it is commonly referred to as the "M2" section. The test circuit area has two primary responsibilities: a) PTH reliability testing of the plated via structures, b) Robustness testing of the materials, during and following assembly. The via reliability protocol involves the electrically (ohmic) heating of the coupon on the IST test system, in order to thermally cycle between ambient and 150°C in 3 minute cycles to measure via reliability.

Figure 9 illustrates the M2 section, it is designed with a "super-heat" circuit (associated to the four-pin connector "B1"), located at four internal levels (layers 3, 7, 14 and 18) within the product construction. The traditional via reliability test (sensing) circuit (four-pin connector "B2") measures the plated through vias from the top to the bottom layers. Area "B3" defines the grid, this study used two separate designs (0.8mm/.032" and 1mm/.040" grid).

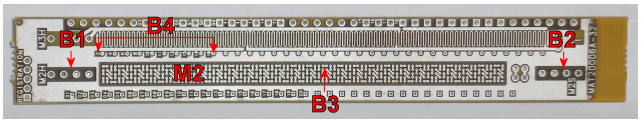

Figure 9: IST Coupon Showing Test Circuits

The B3 section included 0.25mm/0.010" PTH with a grid of either 0.8mm/0.032" or 1mm/0.040". These grid sizes are consistent to the majority of SMT device (PGA, BGA, FPGA, CCGA, etc.) used in today's electronic product, although the 0.65mm/0.0265" grid is starting to become increasingly used. The capacitance holes ("B4") are connected to each of the internal copper planes (plates). The layer to layer configuration selected by the consortium used a strip-line (sig/plane/sig/etc.) concept; each internal copper plane was connected using a drilled PTH, which resulted in 10 internal plates, see figure 10. The image illustrates an example of a plane configuration for making the 9 individual capacitance measurements.

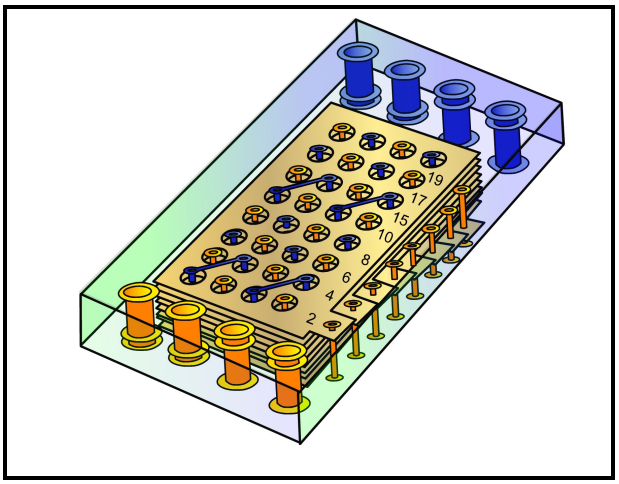

Figure 10: DELAM Plates in IST Coupon

In this study, assembly activities were completed at Celestica Toronto, making the logistics for re-measuring the IST coupon capacitance between and after the 6 reflow cycles possible. Data was collected following exposure to the 2nd, 3rd, 4th and 6th reflow cycles to 260°C. A total of 10 test boards from all 24 material constructions (total 240 test boards) received simulated assembly. After each pass through the reflow oven the test boards were cooled on a rack to ambient. The total time involved in completing all 6 cycles through the reflow oven was 2 days. In order to avoid any additional interruption to Celestica's production schedule it was only possible to re-measure 5 of the 0.8mm/0.032" coupons, after each pass through the reflow oven. After the 2nd, 3rd and 4th assembly cycle the IST coupons were submitted for re-measurement on the automated fixture. Following the 6th cycle 8 coupons from the 0.8mm/.032" and 1mm/.040" coupons were re-measured (2 of the 10 coupons of each type were sacrificed for failure analysis purposes).

Table 3 is an overview of the DELAM results, identifying if a capacitance change greater than 4% were measured after incremental passes through the SMT reflow oven.

The first capacitance measurements were completed after the 2nd reflow cycle, the results identified that all 5 coupons from 3 materials (F, FB and JB) reached the "failure criteria", signifying that material delamination was present. Two reflow cycles would be considered the absolute minimum requirement for assembly, the three materials (F, FB and JB) that delaminated after only 2 reflow cycles would be considered absolutely unacceptable for higher layer products requiring Pb free assembly.

Table 3: Number of Reflow Cycles and when material measured greater than 4% change (Damage) occurred.

IST Coupons Exhibiting Material Degradation (Delamination) Between/After 6X 260°C Reflow Cycles					
Assembly Level	2X Reflow Cycle (Out of 5)	3X Reflow Cycle (Out of 5)	4X Reflow Cycle (Out of 5)	6X Reflow Cycle (Out of 8)	6X Reflow Cycle Only
	Minimum	Standard	One Rework	BGA Rework	BGA Rework
Material Code	.032" / 0.8mm Coupons				.040" / 1mm
FR4:					
A	0	0	0	0	No
AB	0	0	0	0	No
B	0	0	0	0	No
BB	0	0	0	0	No
Halogen Free FR4:					
C	0	40%	80%	88%	No
CB	0	80%	80%	100%	No
D	0	20%	40%	100%	No
DB	0	0	60%	100%	Yes
E	0	0	0	0	No
EB	0	0	20%	100%	Yes
F	100%	100%	100%	100%	Yes
FB	100%	100%	100%	100%	Yes
G	0	40%	40%	50%	No
GB	0	20%	80%	100%	Yes
H	0	0	0	0	No
HB	0	0	0	0	No
High Speed Materials:					
I	0	0	0	100%	No
IB	0	20%	100%	100%	Yes
J	0	60%	100%	100%	No
JB	100%	100%	100%	100%	Yes
K	0	0	0	65%	No
KB	0	0	0	88%	No
L	0	0	0	0	No
LB	0	0	0	0	No
Defective Materials	3	10	12	15	8

Measurements completed after the 3rd pass confirmed the number of failing materials dramatically increased to 10, although only certain numbers (not all) of test boards exhibited material damage. Increased capacitance change was confirmed on the original 3 materials signifying, further damage was caused.

Note: One test board out of the five measuring a greater than 4% change would equate to 20% failure rate, 2 out of 5 would be 40%, etc. Measuring material damage during the 3rd cycle raises major concerns, this level of assembly is considered "normal" for double sided SMT products that require localized attachment, wave soldering, or hand soldering.

The 4th pass through the reflow oven resulted in two additional materials measuring the onset of damage, bringing the total to 12 of the 24 constructions (50%) confirming various degrees of material degradation. The 5th pass could not be measured due to time constraints.

The coupon quantity measured after the 6th cycle (final pass) was increased from a sample size of 5 up to 8. The total number of materials that exhibited damage in the 0.8mm/0.032" grid coupons resulted in 15 of the 24 materials (63%). Within the 15 failing materials 11 measured delamination in all 8 test boards

Following a review of the DELAM results it was agreed by the consortium that if capacitance testing on the IST coupons identified material delamination after the 6X reflow, a quantity of suspect coupons would be cross-sectioned to confirm (or refute) the presence of the material damage.

Upon completion, a review of the combined results (electrical and microsections) a decision was made to go forward with all material types into the via reliability testing phase, with the knowledge that a large number of materials exhibited delamination.

Following the completion of 6X 260°C preconditioning at Celestica the various coupon types were separated from the test boards and sent to their respective test labs for evaluation (Via reliability, CAF, electrical properties, DMA/TMA materials analysis and failure analysis). DELAM testing was completed on the 1mm/0.040" grid coupons; the measured capacitance data determined the presence of material damage in 7 of the 24 materials (29%).

In the case of the 1mm/0.040 coupons the 4% or greater criterion was established from a baseline calculated from the available non-stressed coupons. The ability to apply the DELAM methodology is ideally premised on measuring the same coupon before, during and after exposure to assembly. Using an "averaging" of similar non-stressed coupons is possible, but sensitivity to measure absolute change is limited.

Table 4 shows an overview of the combined results from both DELAM and microsection analysis. The results of all testing were reported to the membership of the HDPUG Pb Free Materials Task Group. The consensus of the membership was overall disappointment that a total of 15 different types of 0.8mm/0.032" coupons from the original 24 materials exhibited material damage after exposure to the 6X assembly cycles. Despite the poor results it was decided to continue with all aspects of material testing, with the knowledge that material damage was potentially present in test vehicles, specifically those that include via structures on a 0.8mm/0.032" grid. The basis of the decision was to understand whether material damage would impact/ or influence via reliability or CAF results.

Table 4: Material Damage Overview

Presence of Material Damage		
Material Type	**.032" Grid**	**.040" Grid**
FR4:		
A	None	None
AB	None	None
B	None	None
BB	None	None
Halogen Free FR4:		
C	Present	None
CB	Present	None
D	Present	None
DB	Present	Present
E	None	None
EB	Present	Present
F	Present	Present
FB	Present	Present
G	Present	None
GB	Present	Present
H	None	None
HB	None	None
High Speed Materials:		
I	Present	None
IB	Present	Present
J	Present	None
JB	Present	Present
K	Present	None
KB	Present	None
L	None	None
LB	None	None
Damaged Material	**15/24**	**8/24**

Failure Analysis After 6X 260C

The next phase of material survivability testing included two in-depth independent assessments by microsection analysis to confirm/refute and better understand the results of DELAM testing. Two stressed and two non-stressed IST coupons from both the 0.8mm/0.032" and 1mm/0.040" (total 8) from all 24 material constructions were sent for failure analysis at Viasystems in China and PWB Interconnect Solutions Inc. (PWBI), in Canada. Both labs microsectioned and analyzed one coupon from each variable to determine whether the non-stress coupon exhibited material issues prior to assembly and the stress coupons to establish the degree to which material damage was present

Effectively both failure analysis labs achieved virtually identical results. The collated analysis completed by Viasystems and PWBI was extensive; with data collected on the presence, type, location and quantity of material damage, drilled hole quality and copper plating thickness measurements. Table 5 identifies the results of combined microsection analysis comparing of the results of DELAM to microsections.

To simplify the correlation the results of each microsection were individually compared to the two capacitance methods. If results reached the same conclusion for finding delamination the data was confirmed to "match", if a disagreement between results was given, the results was confirmed as a "no match". The DELAM method achieved 47 of 48 results with a match (98%) and 1 result with a no match (Material "D" 1mm/0.040" grid).

The comparison of results between DELAM and microsection analysis confirms a very high confidence (98%) that the automated capacitance measurement technique can effectively detect the presence of material degradation.

Table 5: Correlation between DELAM and Microsection After 6X 260°C in Reflow Oven

EMPPS Code	DELAM 1mm	X section 1mm	Match	DELAM 0.8mm	X section 0.8mm	Match
FR4:						
A	No	No		No	No	
AB	No	No		No	No	
B	No	No		No	No	
BB	No	No		No	No	
Halogen Free FR4:						
C	No	Minor		Match	Match	
CB	No	Minor		Match	Match	
D	No	Match	No Match	Match	Match	
DB	Match	Match		Match	Match	
E	No	No		No	No	
EB	Match	Match		Match	Match	
F	Match	Match		Match	Match	
FB	Match	Match		Match	Match	
G	No	No		Match	Match	
GB	Match	Match		Match	Match	
H	No	No		No	No	
HB	No	No		No	No	
High Speed Materials:						
I	No	Minor		Match	Match	
IB	Match	Match		Match	Match	
J	No	No		Match	Match	
JB	Match	Match		Match	Match	
K	No	No		Match	Match	
KB	No	Minor		Match	Match	
L	No	No		No	No	
LB	No	No		No	No	
Results	**23 Match 1 No Match**			**24 Match 0 No Match**		

To further understand the significance of the high correlation achieved between DELAM and traditional microsectioning, Viasystems completed additional analysis by subjecting non-stressed samples to the IPC Thermal Stress (Solder float) methodology. IPC TM 650, Method 2.6.8 was applied, using the industry standard practice of six individual solder floats, for 10 seconds, at a solder temperature of 288C, followed by microsection analysis.

The samples were visually examined using the same approach applied to the previously examined 6X 260C reflow oven stressed coupons. Table 6 confirms the results from the microsections examined after 6X 260C reflow oven compared to samples that received 6X 288C solder floats. The table includes the number of holes examined, a statement of whether delamination was found and the number of cracks found in the sample.

The results for the 48 samples analyzed after the 6X 288C solder float method achieved 32 results with a match (67%) and 16 results with a no match. The poor results are further compounded by the inconsistencies found using the solder float method. In some cases the solder floats caused delamination (more aggressive) in materials that did not delaminate after 6X reflow cycles.

To the opposite extreme, the solder floats were less aggressive and did not find material damage in materials that failed prematurely in the reflow oven, found by both the DELAM methodology and microsection analysis completed after the 6 cycles through the reflow oven.

Table 6: Solder Float (6X288°C) Vs Reflow Oven (6X260°C)

EMPPS Code	6X 260C SMT REFLOW OR 6X 288C SOLDER FLOAT	0.8mm/.032"				1mm/.040"			
		Hole Qty Examined	Delam (15)	Delam Cracks	Match	Hole Qty Examined	Delam (8)	Delam Cracks	Match
A	6X Reflow	13	no	0		11	no	0	
	6X Solder Float	23	no	0		17	no	0	
AB	6X Reflow	16	no	0	No	12	no	0	
	6X Solder Float	24	Yes	1		19	no	0	
B	6X Reflow	15	no	0		12	no	0	
	6X Solder Float	24	no	0		19	no	0	
BB	6X Reflow	16	no	0	No	13	no	0	
	6X Solder Float	23	Yes	1		19	no	0	
C	6X Reflow	17	Yes	9	No	11	no	0	
	6X Solder Float	24	no	0		20	no	0	
CB	6X Reflow	16	Yes	14		14	no	0	
	6X Solder Float	24	Yes	2		19	no	0	
D	6X Reflow	14	Yes	17		12	Yes	10	No
	6X Solder Float	24	Yes	3		20	no	0	
DB	6X Reflow	15	Yes	13	No	12	Yes	7	No
	6X Solder Float	23	no	0		19	no	0	
E	6X Reflow	14	no	0		13	no	0	
	6X Solder Float	24	no	0		20	no	0	
EB	6X Reflow	15	Yes	15	No	12	no	0	
	6X Solder Float	24	no	0		19	no	0	
F	6X Reflow	14	Yes	18		13	Yes	12	
	6X Solder Float	23	Yes	21		18	Yes	28	
FB	6X Reflow	15	Yes	23		12	Yes	13	
	6X Solder Float	25	Yes	22		19	Yes	6	
G	6X Reflow	15	Yes	13		13	no	0	No
	6X Solder Float	23	Yes	21		18	Yes	2	
GB	6X Reflow	15	Yes	15		12	Yes	2	No
	6X Solder Float	23	Yes	1		19	no	0	
H	6X Reflow	15	no	0		12	no	0	
	6X Solder Float	24	no	0		19	no	0	
HB	6X Reflow	15	no	0		13	no	0	
	6X Solder Float	20	no	0		18	no	0	
I	6X Reflow	15	Yes	15	No	12	no	0	
	6X Solder Float	20	no	no		20	no	0	
IB	6X Reflow	15	Yes	15	No	13	Yes	6	No
	6X Solder Float	24	no	0		18	no	0	
J	6X Reflow	15	Yes	16	No	14	no	0	
	6X Solder Float	23	no	0		18	no	0	
JB	6X Reflow	16	Yes	18	No	13	Yes	13	No
	6X Solder Float	24	no	0		19	no	0	
K	6X Reflow	16	no	0	No	13	no	0	
	6X Solder Float	23	Yes	2		19	no	0	
KB	6X Reflow	16	no	0		12	no	0	
	6X Solder Float	23	no	0		19	no	0	
L	6X Reflow	15	no	0		13	no	0	
	6X Solder Float	24	no	0		20	no	0	
LB	6X Reflow	16	no	0		12	no	0	
	6X Solder Float	23	no	0		19	no	0	
Results		14 Match 10 No Match				18 Match 6 No Match			

Table 6 illustrates that material delamination was only confirmed in 6 materials following exposure to 6X 288°C solder floats, for the 0.8mm/.032" grid and 2 materials for the 1mm/.040" grid. Many of the solder float microsection results contradict the microsection results from coupons that experienced 6 passes through the SMT reflow oven.

The dynamic differences between the two types of thermal excursion bring into question whether the 10 seconds of immersion on molten solder (creating an immediate thermal stress to 288C, similar to wave soldering) is representative of each reflow cycles, which experiences 4 to 6 minutes inside the oven, with 60 to 90 seconds of that time above liquidus (see table 2 for reflow oven conditions).

The IPC has established an alternative methodology (Method 2.6.27). No correlation data to reflow ovens is available, but it is considered that this methodology is more representative of a reflow oven profile and should achieve improved ability to predict (by microsection) the presence of material damage.

To further understand the significance of the high level of correlation achieved with the DELAM method to predicting the magnitude of material damage, the study completed additional analysis focused on identifying the specific locations and magnitude of damage within each materials constructions.

Figure 11 illustrates the locations of the layers that receive a capacitance measurement across the internal dielectrics. The majority of dielectrics (Qty 8) are a combined B and C stage pair; the exception is the single C stage (laminate) between layers 10 and 11.

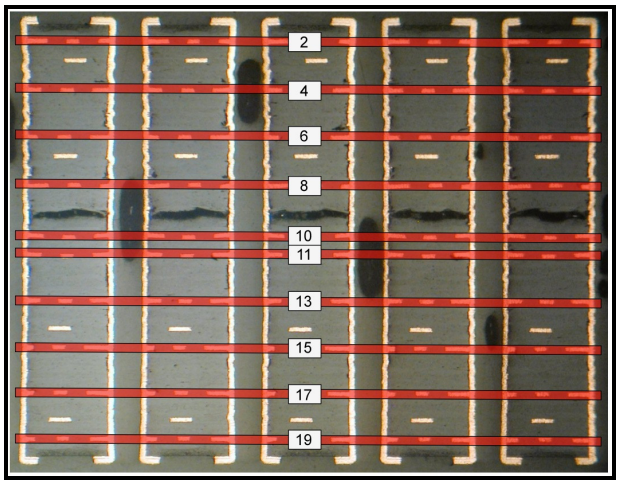

Figure 11: Locations of DELAM Measurements

All 0.8mm/0.032" "stressed" coupons (Qty 192) were measured for bulk capacitance of the 9 dielectrics using the DELAM tester, before the 24 constructions were processing through the SMT reflow oven. Subsequently data was collected on 5 of the 8 coupons after the 2nd, 3rd, 4th pass and all 8 coupons after the 6th pass through the oven. Following the completion of all simulated assembly activities the data was analyzed to identify not only whether damage was present, but just as importantly how much damage and where the damage had occurred.

The following series of graphs demonstrate the measured capacitance data associated to type "A" material, which performed without delaminating, after 6 passes through the reflow oven. As a contrast, material CB which exhibited damage in only the 3rd pass through the reflow oven. Graphs 1a, 2a, 3a and 4a are from material type "A" (FR4 High Tg). Graphs 1b, 2b, 3b and 4b are from material type "CB" (Halogen Free High Tg). The graphs are from the five coupons that were measured at Celestica after cycles 2, 3, 4 and the eight coupons measured after the final pass. A line is included in each graph denoting the 4% criteria applied for identifying material damage.

Graph 1a: Material A - 2nd Reflow No Damage

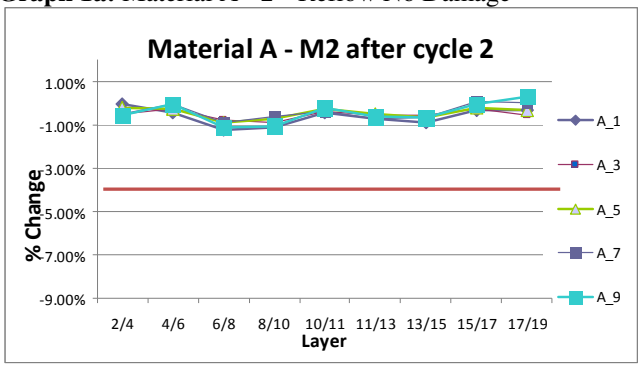

Graph 2a: Material A - 3rd Reflow No Damage

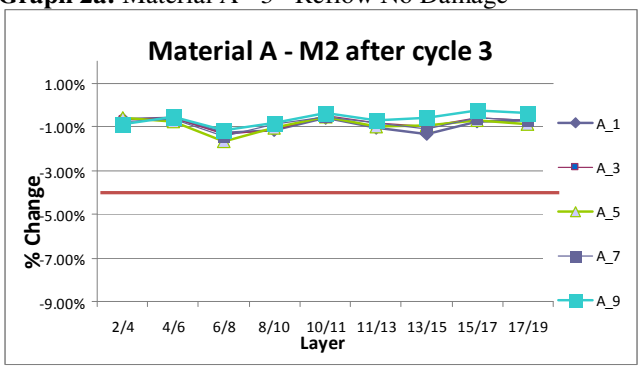

Graph 3a: Material A - 4th Reflow No Damage

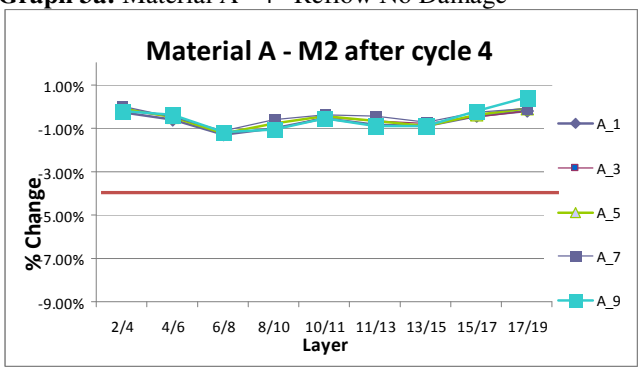

Graph 4a: Material A - 6th Reflow No Damage

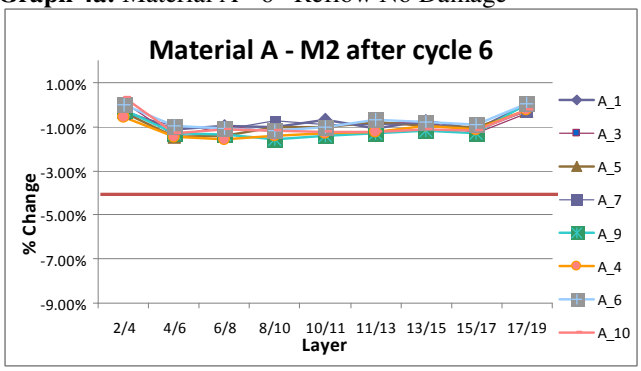

Graph 1b: Material CB - 2nd Reflow with Damage

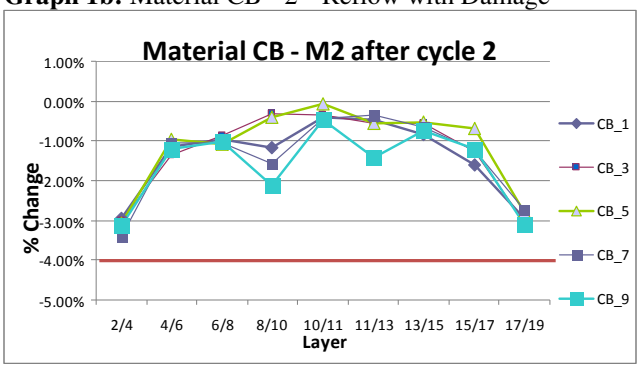

Graph 2b: Material CB - 3rd Reflow with Damage

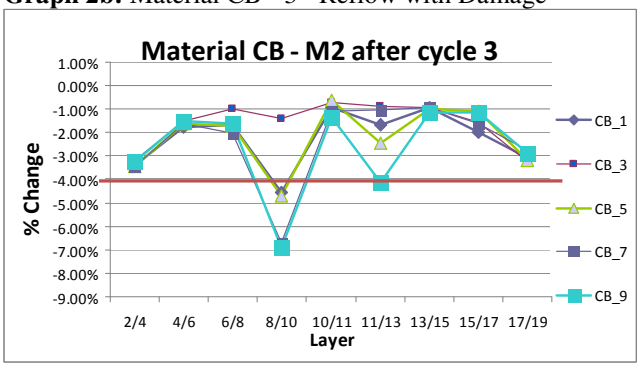

Graph 3b: Material CB - 4th Reflow with Damage

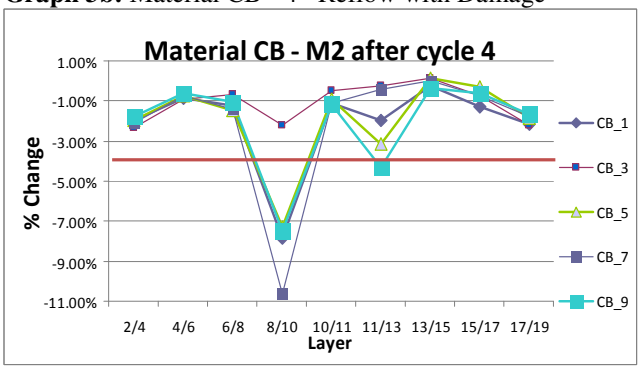

Graph 4b: Material CB - 6th Reflow with Damage

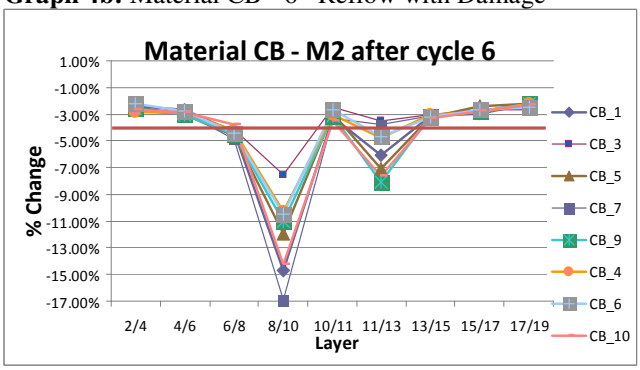

The four graphs associated to material "A" are virtually unchanged, confirming a robust material. The data does confirm a 1% reduction in bulk capacitance throughout the construction; this level of change is related to the inherent moisture removal and is considered normal for this type of construction.

Graph 1b illustrates the relative capacitance change measured in material "CB" after the 2nd pass through the reflow oven. The data shows a curvature conversion to the profile, with the outer layers exhibiting the highest change. Layers 8 to 10 measure a maximum of 2% reduction; layers 11 to 13 measured a 1% change. This small level of change is not classified as delamination, but it is an indicator that damage initiation has started. Graph 2b shows the measurements after the 3rd cycles, it confirms that the previous cycle damage initiation has now propagated into a delamination in 4 of the 5 coupons, between layers 8 and 10, compared to 1 coupon delaminating between layers 11 and 13.

The 4th pass through the reflow oven (graph 3b) increased the maximum capacitance change from a level of 7% up to 11%, effectively quantifying the progressive damage accumulation within the dielectric. Interestingly, the dielectric between layers 11 and 13 were not showing a equal level of degradation, it is considered that the initial crack sites in layers 8 and 10 create a stress relieving influence within the remainder of the construction.

The results of the combined 5th and 6th pass through the reflow oven (graph 4b) confirmed that major material damage would be expected in layers 8 to 10 and lower levels between layers 11 and 13. The magnitude of damage increased to a maximum of 17% change, signifying a "massive" breakdown in the dielectric material. Subsequent microsection analysis confirmed 14 of the 15 dielectrics (between the 16 holes examined) confirmed the presence of major delamination between layers 8 and 10.

An important consideration must be emphasized at this point. The coupons from the 15 materials with known damage did not exhibit any outward signs of the conditions present inside the construction. The unsuspecting user of this product would have no basis for questioning the integrity of the materials.

Capacitance graphs for each individual reflow cycle measured and the associated microsection analysis were collated into 24 individual reports and submitted to the HDPUG Pb Free Materials Task Group for review. Each report was made available to the appropriate material vendor that submitted B and C stage laminates into this study.

A material damage "crack count" was undertaken on all microsections (48 at each of 2 test labs), an overview of the 0.8mm/0.032" grid results are shown in table 7. The numbers of cracks were counted and categorized based on the location and magnitude (size) of the crack. Small sporadic cracks adjacent the edge of the drilled side wall that did not penetrate toward the central zone, were entered under the column "S". Medium sized cracks (M) were classified as a delamination that extended from the sidewall into the central zone. Large cracks that traversed the dielectric between the holes, were entered under column "L". If there were no significant cracks a "0" was entered.

Based on the capacitance measurements results of all 0.8mm/0.032" coupons that completed the 6 passes through the reflow oven, a comparison was made to the 3 levels of material damage found in the microsections. If a check mark "✓" is indicated it confirms that correlation was achieved between the two measurement techniques. An "X" indicates that what was observed and the electrical results were in conflict. There were 68 out of 71 cases where the DELAM electrical data and the crack count correlated. There were three results with a discrepancy between the crack count and the electrical data. The three results were in locations that were not consistent with the common failure sites. The damage found was classified as small, it is considered that the damage did not pass between areas of adjacent internal copper planes and was not measureable within the bulk capacitance.

A crack count was also undertaken on the 1mm/.040" grid coupons (table 8). In the case of the 1mm/.040" grid design the individual coupons were not measured in the "non-stressed" condition prior to the 6X 260C reflow cycles. Without the non-stressed reference if is difficult to correlate the delta capacitance measurements to the observed delamination in the microsections.

The data confirms much smaller number of total material cracks were visible in the 1mm/.040" grid (340) compared to the 0.8mm/.032" grid, (879).

Table 7: Crack Count - 0.8mm/.032" Grid

Crack Count vs. Electrical Data on .032"/0.8mm Grid Coupons																																				
Layer	2/4				4/6				6/8				8/10				10/11				11/13				13/15				15/17				17/19			
R32 Coupons	S	M	L		S	M	L		S	M	L		S	M	L		S	M	L		S	M	L		S	M	L		S	M	L		S	M	L	
A	0	0	0		0	0	0		0	0	0		0	0	0		0	0	0		0	0	0		0	0	0		0	0	0		0	0	0	
AB	0	0	0		0	0	0		0	0	0		0	0	0		0	0	0		0	0	0		0	0	0		0	0	0		0	0	0	
B	0	0	0		0	0	0		0	0	0		0	0	0		0	0	0		0	0	0		0	0	0		0	0	0		0	0	0	
BB	0	0	0		0	0	0		0	0	0		0	0	0		0	0	0		0	0	0		0	0	0		0	0	0		0	0	0	
C	0	0	0		0	0	0		0	0	0		0	0	8	✓	1	0	0	✓	0	0	23	✓	0	8	0	✓	0	0	0		0	0	0	
CB	0	0	0		0	0	0		2	0	2	✓	0	1	28	✓	0	0	0		2	0	1	✓	0	0	1	✓	0	0	0		0	0	0	
D	0	0	0		0	0	0		6	1	0	✓	0	2	10	✓	0	0	10	✓	1	0	3	✓	0	0	0		0	0	0		0	0	0	
DB	0	0	0		0	0	0		0	1	0	✓	0	2	14	✓	0	2	3	✓	0	5	16	✓	0	5	1	✓	0	0	0		0	0	0	
E	0	0	0		0	0	0		0	0	0		0	0	0		0	0	0		0	0	0		0	0	0		0	0	0		0	0	0	
EB	0	0	0		0	0	0		0	4	4	✓	0	0	18	✓	0	0	0		2	0	19	✓	5	0	9	✓	0	0	0		0	0	0	
F	0	0	0		10	0	0	X	0	6	7	✓	0	3	12	✓	0	0	0		0	0	32	✓	12	0	0	✓	0	0	0		0	0	0	
FB	13	0	0	X	22	2	0	X	13	0	3	✓	0	2	14	✓	0	0	0		0	3	20	✓	4	0	0	✓	0	0	0		0	0	0	
G	0	0	0		0	0	0		0	0	0		0	5	9	✓	0	3	4	✓	0	0	7	✓	2	1	2	✓	0	0	0		0	0	0	
GB	0	0	0		0	0	0		12	4	1	✓	0	2	25	✓	0	1	3	✓	0	12	7	✓	7	0	0	✓	0	0	0		0	0	0	
H	0	0	0		0	0	0		0	0	0		0	0	0		0	0	0	0	0	0	0		0	0	0		0	0	0		0	0	0	
HB	0	0	0		0	0	0		0	0	0		0	0	0		0	0	0	0	0	0	0		0	0	0		0	0	0		0	0	0	
I	0	0	0		0	0	0		1		1	✓	0	0	5	✓	0	0	0	0	0	3	10	✓		0	5	✓	0	0	0		0	0	0	
IB	0	0	0		0	0	0		0	4	5	✓	0	6	18	✓	7	0	1	✓	0	0	28	✓	2	0	0	✓	0	0	0		0	0	0	
J	0	0	0		0	0	0		0	0	6	✓	27	0	0	✓	19	0	0	✓	0	0	31	✓	7	0	0	✓	0	0	0		0	0	0	
JB	0	0	0		0	0	0		8	1		✓	32	0	0	✓	23	0	0	✓	1	0	27	✓	0	0	7	✓	0	0	0		0	0	0	
K	0	0	0		0	0	0		0	0	0		6	0	7	✓	1	0	0	✓	0	0	12	✓	0	0	12	✓	0	0	0		0	0	0	
KB	0	0	0		0	0	0		1	0	0	✓	15	0	2	✓	0	0	0		0	0	31	✓	2	0	0	✓	0	0	0		0	0	0	
L	0	0	0		0	0	0		0	0	0		0	0	0		0	0	0		0	0	0		0	0	0		0	0	0		0	0	0	
LB	0	0	0		0	0	0		0	0	0		0	0	0		0	0	0		0	0	0		0	0	0		0	0	0		0	0	0	
Note:	A check mark ✓ indicates the demage in the microsection and the electrical damage agree. An X indicates a disagreement.																																			

Table 8: Crack Count - 1mm/.040" Grid

Crack Count vs. Electrical Data on .040"/1.0mm Grid Coupons																											
Layer	2/4			4/6			6/8			8/10			10/11			11/13			13/15			15/17			17/19		
.040"/1.0mm	S	M	L	S	M	L	S	M	L	S	M	L	S	M	L	S	M	L	S	M	L	S	M	L	S	M	L
A	0	0	0	0	0	0	0	0	0	0	0	0	0	0	0	0	0	0	0	0	0	0	0	0	0	0	0
AB	0	0	0	0	0	0	0	0	0	0	0	0	0	0	0	0	0	0	0	0	0	0	0	0	0	0	0
B	0	0	0	0	0	0	0	0	0	0	0	0	0	0	0	0	0	0	0	0	0	0	0	0	0	0	0
BB	0	0	0	0	0	0	0	0	0	0	0	0	0	0	0	0	0	0	0	0	0	0	0	0	0	0	0
C	0	0	0	0	0	0	0	0	0	0	0	0	0	0	0	0	0	0	0	0	0	0	0	0	0	0	0
CB	0	0	0	0	0	0	0	0	0	0	0	0	0	0	0	0	0	0	0	0	0	0	0	0	0	0	0
D	0	0	0	0	0	0	0	0	0	3	1	0	4	0	0	0	0	0	0	0	0	0	0	0	0	0	0
DB	0	0	0	0	0	0	10	3	1	4	0	19	0	0	0	8	2	3	1	0	0	0	0	0	0	0	0
E	0	0	0	0	0	0	0	0	0	0	0	0	0	0	0	0	0	0	0	0	0	0	0	0	0	0	0
EB	0	0	0	0	0	0	15	4	0	6	3	0	0	0	0	14	8	2	12	6	0	0	0	0	0	0	0
F	0	0	0	0	0	0	4	0	0	1	0	22	0	0	0	2	1	9	13	3	3	0	0	0	0	0	0
FB	0	0	0	0	0	0	10	1	3	5	0	12	0	0	0	6	1	15	5	0	0	0	0	0	0	0	0
G	0	0	0	0	0	0	0	0	0	0	0	0	0	0	0	0	0	0	0	0	0	0	0	0	0	0	0
GB	0	0	0	0	0	0	3	3	0	12	0	0	7	0	0	4	3	0	4	0	0	0	0	0	0	0	0
H	0	0	0	0	0	0	0	0	0	0	0	0	0	0	0	0	0	0	0	0	0	0	0	0	0	0	0
HB	0	0	0	0	0	0	0	0	0	0	0	0	0	0	0	0	0	0	0	0	0	0	0	0	0	0	0
I	0	0	0	0	0	0	0	0	0	0	0	0	0	0	0	0	0	0	0	0	0	0	0	0	0	0	0
IB	0	0	0	0	0	0	4	0	1	1	0	12	0	0	0	3	0	3	1	0	0	0	0	0	0	0	0
J	0	0	0	0	0	0	0	0	0	0	0	0	0	0	0	0	0	0	0	0	0	0	0	0	0	0	0
JB	0	0	0	0	0	0	8	0	0	0	0	0	0	0	0	1	0	24	1	0	0	0	0	0	0	0	0
K	0	0	0	0	0	0	0	0	0	0	0	0	0	0	0	0	0	0	0	0	0	0	0	0	0	0	0
KB	0	0	0	0	0	0	0	0	0	0	0	0	0	0	0	0	0	0	0	0	0	0	0	0	0	0	0
L	0	0	0	0	0	0	0	0	0	0	0	0	0	0	0	0	0	0	0	0	0	0	0	0	0	0	0
LB	0	0	0	0	0	0	0	0	0	0	0	0	0	0	0	0	0	0	0	0	0	0	0	0	0	0	0
Total Crack	0	0	0	0	0	0	54	11	5	32	4	65	11	0	0	38	15	56	37	9	3	0	0	0	0	0	0

The collation of data collected during the crack count analysis identifies an interesting understanding of where the damage was being created within the product constructions. The trends for damage locations are the same for both grid sizes, but the magnitudes of cracks found in the 24 samples from each grid size are drastically different.

Graphs 5 illustrates the distribution of small, medium and large sizes material cracks for the 0.8mm/0.032" grid coupons. The count is from the 15 materials that delaminated during the 6 cycles through the reflow oven. The data has been sub-divided by the two constructions (58% and 69%) used with each material. The data identifies that the majority of damage, signified by the medium and large cracks is occurring between layer 8 to 10 and layers 11 to 13. The B/C stage pairs are located equally on either side of the central C stage layers (L10/L11). The adjacent B/C stage pairs (L6 to L8 and L13 to L15) experienced relatively much less damage.

Graph 5: 0.8mm/0.032" Crack Distribution

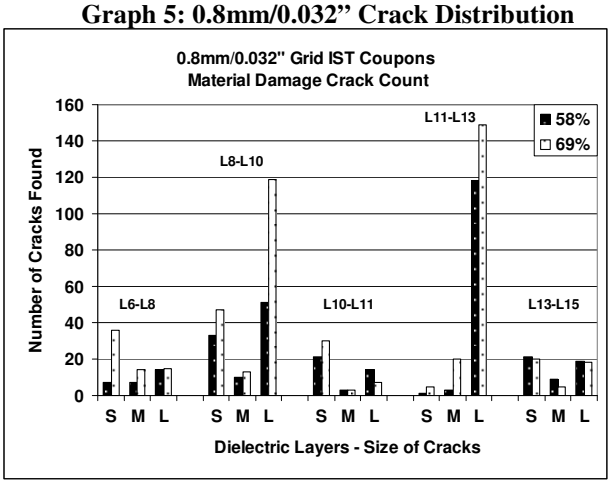

Graph 6 relates to the same 24 materials, but the crack count is based on the 1mm/0.040"grid, for the 8 materials that exhibited delamination. The magnitude of damage is dramatically lower, and interestingly the dominance of the two dielectric pairs (L8 to L10 and L11 to L13) is still apparent, but less obvious.

Graph 6: 1mm/0.040" Crack Distribution

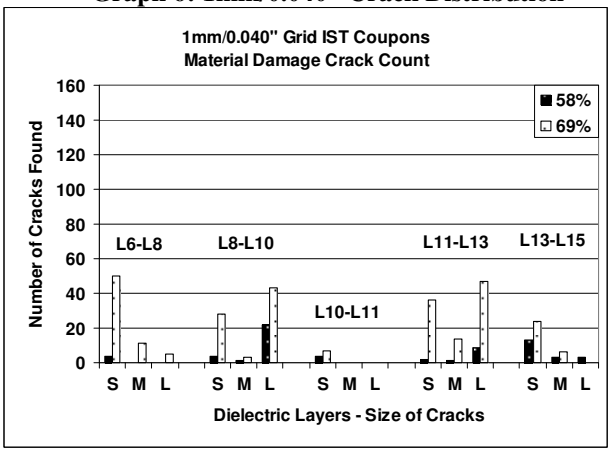

With the reality that everything else in the coupon construction was equal (material type, B & C stage configuration, hole size, plating conditions, etc.) it is extremely important to understand why such a small change in via to via spacing (0.2mm/0.008") has such a significant impact toward the magnitude of material damage created during 6X 260C assembly. The DELAM data has enabled an "electrical map" of the damage distribution throughout the construction. To reach a determination of root cause it is necessary to combine the examination of the microsections with the DELAM data to establish the type and possible reason for the different levels of damage.

Visual examination of the 15 materials from the 0.8mm/0.032" coupons that exhibited material delamination (electrically and in microsections) confirmed that all damage sites were caused by **cohesive** failures. No delamination was found to be caused by an adhesive failure at the bond line between the B and C stage materials, or between B stage and the copper foils. Cohesive cracks are produced within the epoxy, or phenolic C-stage and/or cured B-stage dielectrics layers, specifically at the junctions between the resin and the glass bundles. The crack sites tend to initiate in the central area between the PTH vias, they follow the direction of the glass fabric, but can frequently digress, resulting in multiple smaller cracks. See figure 12 for an animation of cohesive material. Note that the figure is not the same construction and via types used in this study.

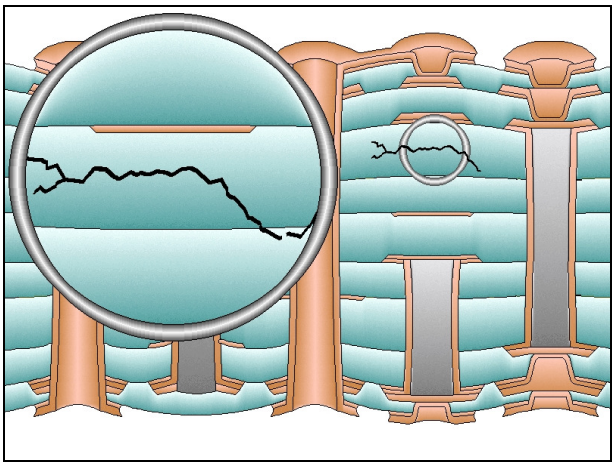

Figure 12. Cohesive Cracking Failure

Figure 13 shows a typical delamination in the cured B stage material between layers 11 and 13, from type "KB" (High speed). The fracture site is initiating in the central zone, on the outer edges of the glass bundles, the cracks are propagating toward the barrels. The two visible B/C stage bonding lines do not exhibit any indication of adhesive breakdown.

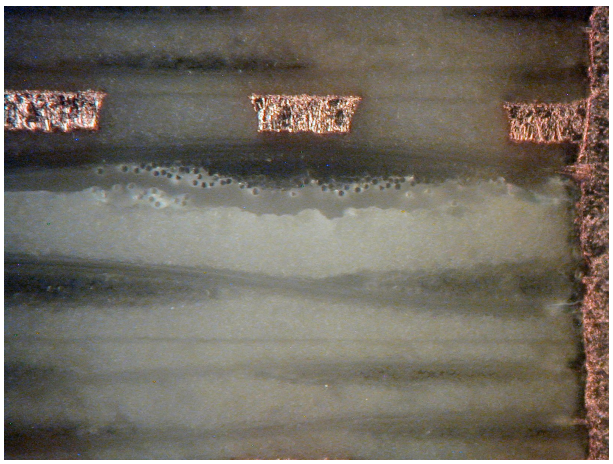

Figure 13: Cohesive Material Damage

In some materials cohesive damage was widespread throughout the construction, see figure 14 for an example of multiple locations exhibiting cohesive failures.

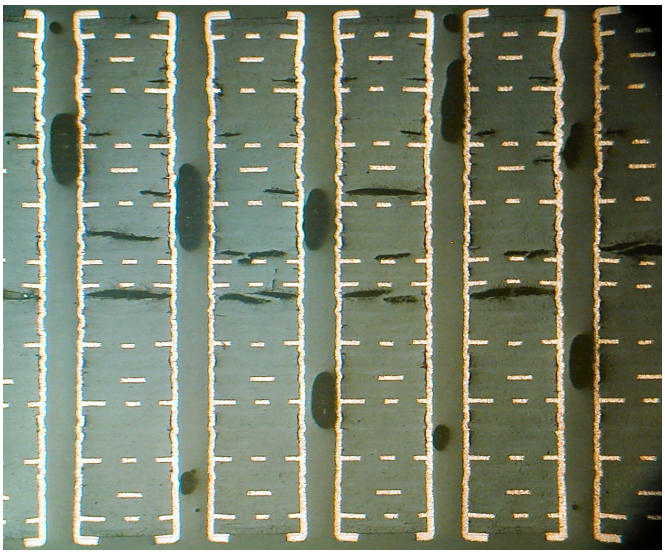

Figure 14: Material "FB" - 0.8mm/.032 Grid

Figure 15 illustrates the results from DELAM testing after 6X 260°C. The data confirms multiple dielectrics exhibited reductions in measured bulk capacitance (up to 14%).

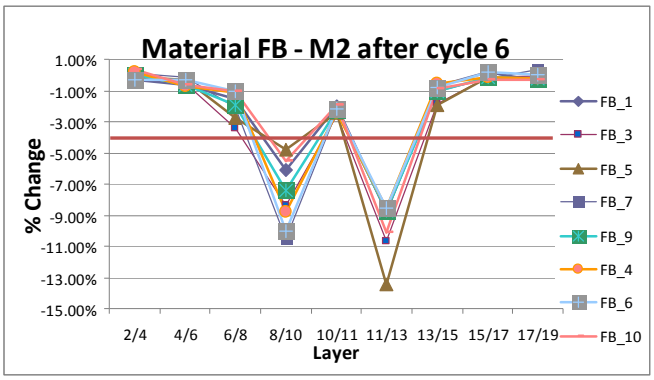

Figure 15: DELAM Data Showing Damage Locations

Knowing that both construction types used 1080 style glass for the B stage; microsections were further analyzed to determine if the glass style was influencing the propensity to cause cohesive delamination. Figure 19 identifies the materials that exhibited the damage within the 58% and 69% resin construction. A single "x" in the construction column means all damage was found in one specific dielectric. If a second "x" is present it means damage was equally distributed between both B and C stage. The data confirms there was no clear trend toward a specific glass type, but the 1080 style B stage did contain cohesive material damage in 12 of the 15 constructions. In 8 of the 12 cases the cohesive damage was only found in the B stage material. In two materials (D and EB) the cohesive damage was related to only C stage material, D material was built with 2116, EB was built with 2X 106 style glass.

Material Type	58%		69%	
	C=1X 2116	B= 2X 1080	C= 2X 106	B= 2X 1080
C		x		
CB				x
D	x			
DB			x	x
EB			x	
F		x		
FB				x
G	x	x		
GB			x	x
I	x	x		
IB			x	x
J		x		
JB				x
K		x		
KB				x

Figure 16: Glass Style Vs Material Damage Found

Figure 16 also identifies the glass fabric supplier associated to each material construction. The glass supplier and the glass fabric type for the 15 materials that delaminated were evenly divided between the two major glass manufacturers (Asahi and Nittobo). Damage was found in all 3 glass styles (2116, 1080, 106), the majority of damage was found in the B stage (2X 1080), which occurred in 13 of 15 constructions.

Based on all of the collated electrical (DELAM) and microsection data, the only remaining "unknown" component is the mechanical strength of the materials that is present between the PTH. To understand this situation it is first necessary to understand the geometries and attributes of the designs and summarize the conclusions of all previous analysis.

The 2 coupon designs have identical layouts, signal/plane configurations, inclusion of non functional pads on the plane layers. The only exception was PTH grid size.

1. The 0.8mm/0.032" and 1mm/0.040" coupons were located immediately next to each other on the same test board, which was stepped and repeated 4-up on the production panel.
2. Both coupons were drilled with 0.25mm/0.010" drills
3. All material constructions (24) were built at one PWB manufacturer (Viasystems in China)
4. Identical conditions were applied to all test boards during processing through the same reflow oven (6 times)
5. Delamination was confirmed in 15 of the 24 materials in the 0.8mm/0.032" grid design, but only 8 materials in the 1mm/0.040" grid.
6. All damage sites exhibited cohesive delamination, the majority of laminate cracks were found in the central zone in both B and C stage materials.
7. No adhesive delamination was found.
8. The location of damage sites within the construction was consistent between the two grid sizes.
9. The magnitude of damage in material types where both grid sizes delaminated (8 types) was between 2X and 10X greater in the 0.8mm/0.032" coupons compared to the 1mm/0.040".coupons
10. The glass fabric manufacturer and glass style did not appear to impact the results.

Why did the 0.8mm/0.032" fail before the 1mm/.040"?
Based on failure analysis the weakest point of adhesion proved to be at the resin to glass interface, consequently the resin to copper and resin to resin bonds demonstrated to be strong enough to withstand the shear stress. The inclusion of non-functional pads decreases the surface area at the resin to resin interface of the B and C stage dielectrics, increasing the shear stress, by locking the resin at the non-functional pad locations. See figures 17 and 18 for geometries associated to the 2 grid sizes. This situation is consistent with decreasing the grid size while maintaining a common hole and pad diameter, as was evident in testing. Despite the grid size and non-functional pads the shear stress is equal, but the strain increases due to the smaller area in the x/y axis.

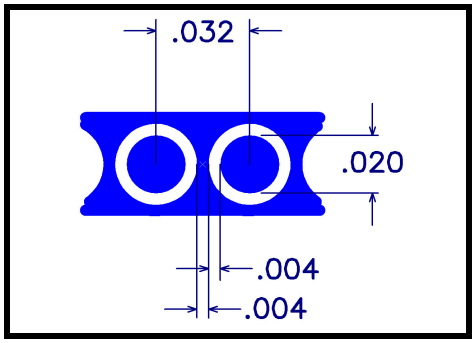

Figure 17

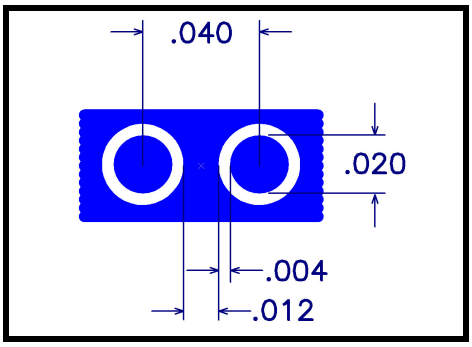

Figure 18

When the structure of the composite materials reaches a specific temperature during each assembly cycle an internal shear stress is generated by the mis-match of CTE. The CTE mismatch is caused by the combination of the strength of the glass restricting the x axis expansion, versus the non-restricted expansion of the resin in the y axis. The focal point of this CTE mismatch is located at the "knuckle" between the woven glass fabrics; this is premised on the examination of microsections that consistently exhibit material cracks at the cross-over point between the warp and the weft glass direction.

Damage initiation is generated during reflow assembly by shear stress fracturing at the silane interface. The silane treatment is designed to promote a strong (unbreakable) chemical bond between glass fibres and the resin system. Following crack initiation damage is further propagated and distended by a torsional stress caused by the z axis expansion, focused on, or between the glass bundles. The nature of the cohesive damage is compromising this critical glass/resin interface, what is uncertain is whether the fracture point is between the resin and silane, or the silane and glass. Information related to which material used what silane treatment is not known to the authors.
Differences in the performances between the glass/resin styles is counter-intuitive, the material with the highest resin content (106) did not exhibit the majority of damage, the material with the largest glass fibres and lowest resin content (2116) did not exhibit the majority of damage. This is possibly due to competing (restrictive and non-restrictive) x/y stresses

Failure analysis confirmed that the majority of cohesive material damage was present within the central zone of the construction. Based on the high temperatures experienced during reflow assembly and each materials inherent thermal conductivity, Tg and CTE, the maximum x/y shear stress is generated at the centre of the construction. Understanding how each materials conductivity, Tg and CTE impact their performance was not compared in this study. Future studies must collect this important data for comparison to determine whether correlation to material damage is found.

Based on the disappointing results achieved in this study the HDPUG consortium have initiated a new materials reliability project, focused on understanding the influence of multiple grid sizes and their effect on material integrity through Pb free assembly. The study will design, build, assemble and DELAM test coupons with 1mm/0.040", 0.9mm/0.036", 0.8mm/0.032", 0.7mm/0.028" and 0.65"/0.0265" grid sizes.

The five grid sizes will be built with 2 constructions of 3 materials types that delaminated on the 0.8mm/0.032" grid, but did not delaminate on the 1mm/0.040" grid. The present scoping of the study could also contain changes to internal plane configuration, in one case using a concentration of multiple planes in the centre of the stack-up.

The DELAM methodology is being enhanced to support IST testing by including the ability to heat the coupons with the same thermal profile created in Pb free assembly reflow ovens. This capability avoids the difficulties in getting access to the ovens, which are in high demand for supporting production. This added functionality will create a very useful tool for the PWB manufacturer, contract manufacturers and OEM's, it will enable an effective non-destructive capability to understand the materials and product constructions ability to survive multiple assembly cycles, without the inconvenience of interrupting reflow oven capacity. Correlation studies will be completed to establish the confidence that the DELAM thermal profile achieves the same results as the reflow oven.

IST Coupon, Designed to measure for Via Reliability

The IST coupons contain a daisy chain of PTH vias used for measuring the plated through hole reliability. There were two design configurations related to via to via spacing (0.8mm/0.032" and 1mm/0.040"). All coupons were constructed on the same test panels, with 20 layers, laminated to an average thickness of 0.115" (2.92mm), both were drilled with 0.010" (0.254mm) vias, producing an aspect ratio of 11.5 to 1. The electrolytic copper thickness was specified to achieve a minimum of 25 microns (0.001"), which was subsequently confirmed through microsection analysis.

Problem Statement

The basis of a successful PTH via reliability study is built upon the premise that material integrity is not compromised, and an assurance that fatigue of the PTH barrel is the only failure mode.

The presence and magnitude of material damage found after 6X 260°C creates a major confounding impact on the ability to complete an effective PTH via reliability study. From the original 24 submissions (12 materials x 2 constructions) only 8 (4 materials) candidates "survived" assembly without moderate to severe material damage.

An accumulation of multiple copper fatigue cracks across the central area of the barrel is the anticipated failure mode for most PTH structures. The presence of material cracks in the same region of the construction can have two primary confounding effects on the measured cycles to failure; 1) Stress Focusing - Cohesive cracks that extend to the edge of the drilled sidewall can initiate cracking within the electroless and electrolytic copper plating's. Once copper cracking has initiated at this isolated location, individual crack propagation becomes accelerated. Stress focusing damage can be determined by the absence of other fatigue cracks in the same barrel. 2) Stress Relieving – The dominant material characteristic that determines how much stress that will be applied to the barrels of a PTH structure is the Coefficient of Thermal Expansion (CTE). The CTE movement is 3 dimensional, with different expansion rates for x and y axis, compared to higher values in z axis. The distribution of the x, y and z axis stresses change when confronted or combined with a situation where material cracks are present. During each thermal cycle the stresses are able to dissipate into the damaged material, thus not be fully directed toward the copper barrel. This situation results in two conditions where extended performance is measured; a) Slower crack propagation, due to the lower strain loading. b) A movement of the damage accumulation to an area away from the material damage. The most common result of this condition effectively divides the barrels into "two half" barrels, stress cracks are found between the surface and central layers, with no cracks present in the middle of the barrel.

Material damage can cause both stress focusing and stress relieving conditions; either situation creates a confounding effect on a quantitative and comparative determination of PTH reliability. Fortunately for the participants of this study, the type, magnitude and locations of the damage condition for each material and design option were recognized, before all levels of testing commenced. Via reliability and CAF testing activities were both impacted due to the presence of PTH vias located on 0.8mm/0.032" and 1mm/0.040" grids, used in their test vehicles. Electrical performance and material analysis used test vehicles that did not contain vias as part of their test circuits and where not impacted by the cohesive damage.

The results of all testing were reported to the membership of the HDPUG Pb Free Materials Task Group. The consensus of the membership was overall disappointment that a total of 15 different types of 0.8mm/0.032" coupons from the original 24 materials exhibited material damage after exposure to the 6X assembly cycles. Despite the poor results it was decided to continue with all aspects of material testing, with the knowledge that material damage was potentially present in test vehicles, specifically those that include via structures on a 0.8mm/0.032" grid. The basis of this study was to understand whether material damage would impact, or influence via reliability results.

IST Testing Methodology and Protocol

The IST coupons were cycled in conformance the IPC-TM-650 Method 2.6.26 Current Induced Thermal Cycling. Heating was achieved by applying a low-level electrical current to the coupons "super-heat" circuit, this heating "element" resides on 4 levels within the construction of the coupon. There is no electrical current passed through the PTH vias, the plated structures are heated passively by the heating circuit. A 10% failure criteria were used, IST test equipment has the ability to stop immediately at the level of 10% increase in the test circuit's bulk resistance (as per IPC Standards). This capability identifies a further advantage of the IST methodology in the fact that each coupon is individually stopped within seconds of reaching the 10% criteria, permitting precise understanding of the damage initiation and accumulation upon microscopic examination.

Throughout IST testing all test circuits are continuously monitored for resistance change, data collection is automated, compared with internal rejection references and displayed simultaneously. Each coupon stops testing upon reaching the rejection criteria, when a coupon is stopped it will not receive any additional stressing, the coupon remains at ambient until removed from the tester. Analyzing all failed coupons at the same level of rejection is critical in relative testing, any additional damage caused after the 10% rejection criteria will confound and confuse failure analysis. The capability to stop stressing at failure is unique to IST, in traditional thermal stress ovens all coupons continue to receive stressing until the maximum number of test cycles is completed.

When each test coupon has reached a 10% increase in bulk resistance, it is a sufficient resistance change to find a cylindrical barrel crack. The test circuit has not progressed to a point of producing an electrically intermittent, or open via. Using a sensitive thermo-graphic camera in consort with the application of a small electrical current into the test circuit, the one or two vias that exhibit the most accumulated damage to the PTH barrel structures are identified and selected for failure analysis.

Sample Size - Test Condition – Number of Cycles

Upon receipt twenty-four coupons of each material type were segregated into their two test conditions, 12 non-stressed and 12 stressed (6X 260°C in reflow oven). Each test condition was sub-divided into the 6 coupons designed with a 0.8mm/0.032" grid and 6 designed with a 1mm/0.040" grid. Each IST cycle was completed from ambient (23°C) to 150°C using three minutes of heating and approximately two minutes of cooling. There are no dwells at either temperature extreme. IST testing was continued until a coupon reached the rejection criteria of a 10% increase in bulk resistance, or to a maximum of 2000 cycles, whichever came first.

IST Resistance (Damage Accumulation) Graphs

Resistance data for each coupon (and test circuit) is collected automatically throughout every heating and cooling cycle. The data from the end of the heating cycles is generally used to show PTH barrel damage accumulation. This allows the user to understand how damage was accumulating during the IST test.

Most coupons in this study showed a slow progressive acceleration curve, indicating high quality copper plating. Example 1 shows coupons from material "JB" (Halogen Free 69%), shown in graph 7, confirm fatigue until approximately 225 to 300 cycles, then exhibit acceleration.

Graph 7

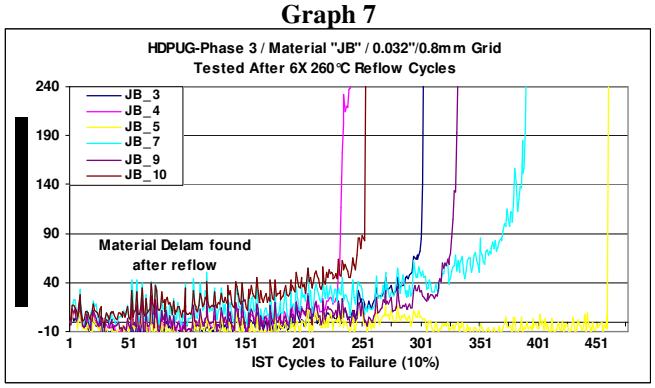

Example 2 are coupons from material "I" (High Speed FR4 58%) illustrated in graph 8, show failure initiated between 300 to 500 cycles, followed by a slow/progressive constant wear-out. This is a typical failure due to metal fatigue.

Graph 8

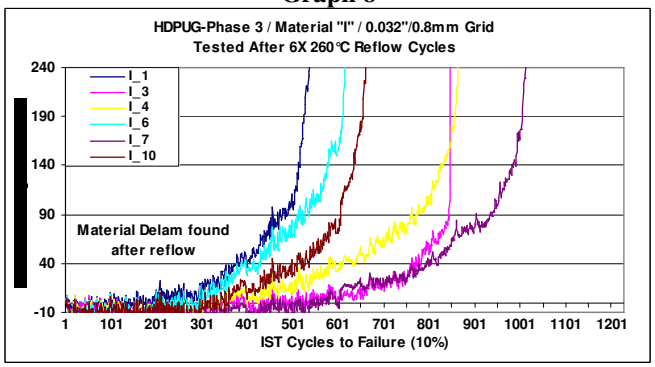

Failure analysis

This phase of analysis proved to be the most intriguing part of the entire via reliability study. It enabled an ability to view the complex interactions that take place between material damage and barrel cracking. One of the main reasons for the complexity is that the barrel cracking should be expected to occur within the central region of the copper plated barrel, this is exactly where the majority of material damage was found after 6X 260°C reflow cycles.

The microsection analysis was completed with the full knowledge that material damage was present in a large quantity of material constructions before IST testing was

initiated. The visual inspection of each section was completed with a focus toward the locations of barrel cracks, relative to the locations of material cracks. It is important to emphasis that the magnitude and locations of cohesive damage (delamination cracks) ranged between materials. In some constructions all cracks were consistently between the same dielectric layers, whereas in other constructions cohesive damage was randomly located across multiple dielectrics.

After IST testing, a representative coupon from each material construction, test condition and grid size were selected for failure analysis. The vias exhibiting the largest resistance change in each coupon were selected for analysis; failure location was achieved by using a thermo-graphic camera. This decision to select the vias with the most damage to the copper plated barrel does not automatically mean that this is also the same location to expect to find the most cohesive damage in the material. There is a complex interaction that causes stress relieving on the vias located near material damage, it should be expected that "lower levels" of damage would be expected in the location of the failing vias.

The initial conclusions from the microsections confirmed the dominant failure mode found in the PTH barrel was due to a copper wear-out type cracks, caused by metal fatigue. The size of cracks found in the sections were all at a point of a 10% increase in test circuit resistance, it is understood that the number of cracks propagated are relative to the number of cycles achieved in IST testing. The cracks generally started at a glass fiber and slowly propagated around the copper crystals.

The major finding during failure analysis was the relationship between the barrel crack locations and the cohesive material damage locations. In materials constructions that did not delaminate during the 6X 260°C reflow cycles, all cracks were consistently found in the B/C stage dielectric pairs (L8 to L10 and L11 to L13) on either side of the central C stage dielectric (L10 to L11). In materials constructions with cohesive material damage present, virtually no copper cracks were found in the same barrel locations. Cracks sites were either located further away from the central layers (L6 to L8 or L13 to L15), or in situation where delamination was present on one side of the construction, all barrel cracks were found on the opposite side. In some instances material damage was located randomly on either side of the central C stage, in each case the copper crack sites were only found on the opposite side of the construction.

Figures 19 and 20 show examples of how cracking in the copper plated barrels propagated on the opposite side of the construction, relative to the location of the cohesive material damage. Photo 2 is from a 0.8mm/0.032" grid coupon built with the "CB" construction (Halogen Free - 69% resin content), the cohesive damage is clearly evident on the upper and lower side the central C stage layers (L10 to L11). If damage was not present copper cracking would be expected in the B/C stage layers on either side(L8 to L10 and L11 to L13). The image shows that the cracks moved outwards into dielectrics further from the central plane (L6 to L8 or L13 to L15).

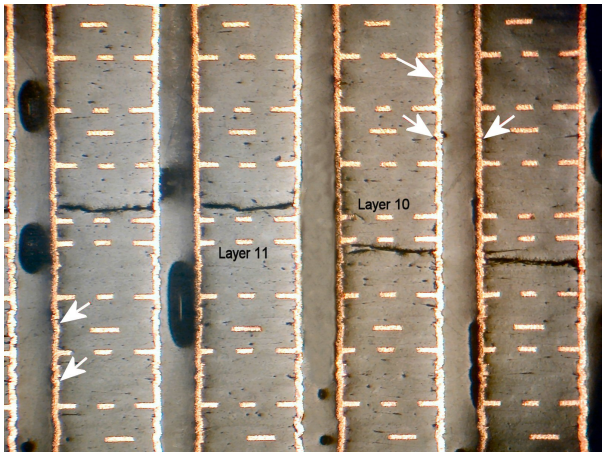

Figure 19 Material "CB"

An important consideration that must be emphasized at this point is that Viasystems China processed excellent copper plating distribution into the test boards, achieving a very uniform thickness throughout the length of the barrel. The presence of cohesive cracks causes the barrel crack to propagate outside of the traditional central zone. The combination of redistributed crack sites with the even copper thickness did not cause an extension to the number of thermal cycles required to achieve the rejection criteria. In situations where a plating taper is present, this is where thicker copper is plated near the surface compared to thinner copper in the centre; in this situation higher cycles to failure would be required to fail the test circuit.

Figure 20 is from a 0.8mm/0.032" grid coupon built with the "GB" construction (Also Halogen Free - 69% resin content), the pattern is repeated, showing a similar re-distribution of barrel cracks relative to the location of the cohesive material damage.

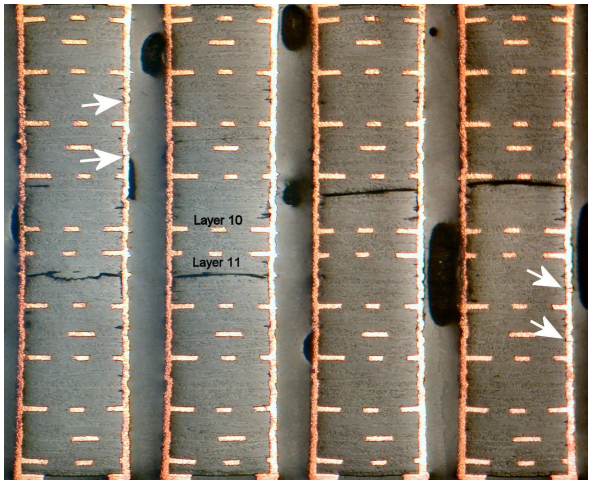

Figure 20 Material "GB"

The results of this analysis in this study confirmed that material damage was stress relieving, copper cracks were effectively redistributed into different locations within the same via structure. This conclusion does not automatically mean that cycles to failure will be greatly extended, but it should be understood that a critical area of the plated barrel will not be contributing to the measurement of damage accumulation. The influence of material integrity can also highly accelerate copper plating damage (stress focusing), in certain situations material integrity can be a dominating influence on PTH via reliability. It is strongly recommended that a combination of methodologies that effectively quantify the conditions associated with the copper plating, in parallel with measurements of material integrity are both essential to completing effective root cause analysis on product failures.

A secondary objective of failure analysis was to determine the failure modes and to help in the identification of any anomalous results. All the failed coupons were confirmed to contain barrel cracks, as shown in the examples in Figures 21 and 22. A total of 24 individual test reports were created and submitted to the HDPUG Pb free materials task group. Each report contained IST resistance graphs, plating thickness measurements, copper crack counts and images of failure sites.

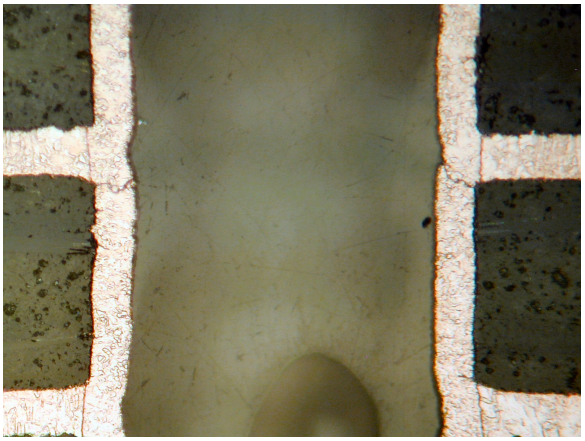

Figure 21

The second type of failure found was a barrel crack with plastic deformation of the dielectric material. In this type of failure mode the crack typically initiates at a glass fiber but go horizontally, progressing through copper crystals. One of the characteristics of this type of failure mode is that the crack is open at ambient and tends to propagate at 90° angle to the barrel. This type of failure was noted on material "H" only. The selected coupon failed after 1161 cycles, this is considered a much extended level of performance and should not be interpreted as a negative aspect of the material performance.

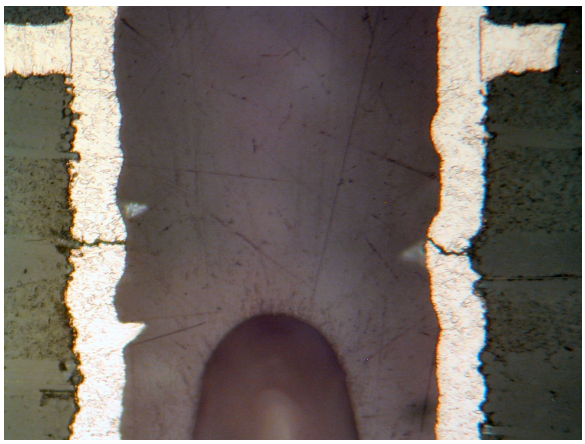

Figure 22

IST Results

The mean IST cycles to failure for each material type, relative to test condition and grid size are represented in Table 9. The results for material's "E" and "EB" are highlighted in red because they achieved a relatively low performance in both the non-stressed and 6X260°C conditions, compared to all other materials. The "Damage" columns confirm which materials exhibited cohesive delamination after the 6X 260°C reflow cycles. Each material's non-stressed results versus 6X 260°C results were compared to determine if the IST cycles to failure for 6X 260°C out-performed the non-stressed results. The seven materials demonstrating this condition all showed delamination after reflow. It is consider that the extended performance is caused by the stress relieving effects of the cohesive delamination. In two of these 7 cases the mean 6X260°C cycles to failure doubled the performance of the same coupons tested non-stressed.

Table 9: Overview of Mean IST Cycles to Failure

EMPPS Coding	1mm/0.040" Grid				0.8mm/0.032" Grid			
	IST 1mm As Built	IST 1mm after 6X 260C	Damage - 1mm	1mm 6X Compare better than AB?	IST 0.8mm As Built	IST 0.8mm after 6X 260C	Damage - 0.8mm	0.8mm 6X Compare better than AB?
High Tg FR4					**High Tg FR4**			
A	677	513	No	No	699	521	No	No
AB	447	358	No	No	420	362	No	No
B	372	256	No	No	332	228	No	No
BB	380	173	No	No	386	201	No	No
Halogen Free					**Halogen Free**			
C	993	568	No	No	932	628	Yes	No
CB	768	393	No	No	805	598	Yes	No
D	516	332	Yes	No	566	289	Yes	No
DB	490	378	Yes	No	499	642	Yes	Yes
E	173	43	No	No	169	16	No	No
EB	115	42	Yes	No	109	53	Yes	No
F	280	527	Yes	Yes	259	558	Yes	Yes
FB	235	381	Yes	Yes	223	260	Yes	Yes
G	>2000	1269	No	No	>2000	1753	Yes	No
GB	>2000	1217	Yes	No	1860	2000	Yes	Yes
H	>2000	>2000	No	No	>2000	1860	No	No
HB	1906	1157	No	No	1955	1032	No	No
High Speed FR4					**High Speed FR4**			
I	1040	576	No	No	962	760	Yes	No
IB	819	374	Yes	No	757	756	Yes	No
J	434	191	No	No	404	333	Yes	No
JB	302	224	Yes	No	280	331	Yes	Yes
K	821	335	No	No	768	392	Yes	No
KB	602	382	No	No	623	385	Yes	No
L	>2000	1703	No	No	>2000	1859	No	No
LB	>2000	1567	No	No	>2000	1730	No	No

Graph 9 gives a graphical representation of the mean cycles to failure for the 0.8mm/0.032" and. 1mm/0.040" grid coupons tested non-stressed and after 6X 260°C.

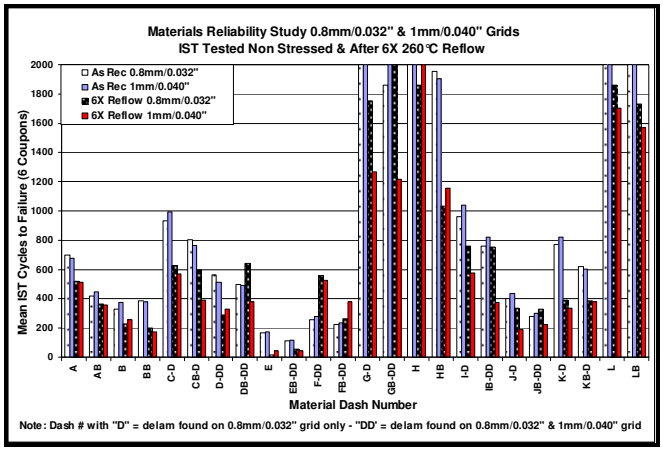

Graph 9

The initial impression confirms a wide variety of performances levels were achieved, from immediate failures to virtually unbreakable. The situation is further complemented by the fact that all material constructions were processed together through the same electrolytic copper plating chemistry, removing the ambiguity and overriding confounding effects. Under ideal conditions it would permit an ability to rank each material, under the pretence that inherent material properties were dominating performance. Unfortunately in this study we must incorporate the reality that 15 of the 24 materials on the 0.8mm/0.032" grid and 8 of the materials on the 1mm/0.040" grid delaminated during assembly.

The following data presented in Tables 10 are an overview of all IST cycles to failure for both test conditions and grid sizes. The data contains standard statistics, a statement identifying if cohesive delamination was found in the 0.8mm/0.032" grid coupons and the lower 90% confidence bound of a log normal distribution. To simplify the relationship between standard deviation and the mean, the log normal analysis will take precedence over standard statistic for all further comparisons between material performances.

One aspect of comparing the non-stressed coupons to the stressed coupons was to determine how much "life" was removed by the 6X 260°C reflow cycles. Based on non-damaged coupons only, the impact of assembly measured a reduction ranging between 38% and 45%. With all damaged materials included the data range reduced to between 23% and 35%. In the majority of cases the "residue life" would be considered sufficient to meet the end use environment requirement, based on most commonly used IST testing specifications.

Table 10

Standard Statistics For 0.8mm/0.032" and 1mm/0.040" Combined											
EMPPS Code	Test Condition	Construction	Mean	Std. Dev.	Min.	Max	Range	Coef. Var		Delam in 0.8mm/0.032"	Lower 90% Log Normal
High Tg FR4											
A	As Built	A	688	93	567	914	347	13%		No	646
AB		AB	433	69	334	581	247	16%		No	402
A	6X260°C	A	517	126	292	659	367	24%		No	453
AB		AB	360	45	284	423	139	13%		No	337
B	As Built	B	352	87	196	487	291	25%		No	852
BB		BB	383	61	305	501	196	16%		No	730
B	6X260°C	B	242	49	151	330	179	20%		No	219
BB		BB	187	63	47	275	228	34%		No	155
Halogen Free Material											
C	As Built	C	963	239	541	1303	762	25%		No	852
CB		CB	786	122	648	1032	384	16%		No	730
C	6X260°C	C	598	248	338	1072	734	41%		Yes	498
CB		CB	495	138	309	703	394	28%		Yes	433
D	As Built	D	541	125	352	750	398	23%		No	482
DB		DB	494	76	337	620	283	15%		No	457
D	6X260°C	D	315	95	154	442	288	30%		Yes	265
DB		DB	510	162	242	797	555	32%		Yes	436
E	As Built	E	171	20	136	196	60	12%		No	160
EB		EB	112	15	90	133	43	14%		No	104
E	6X260°C	E	36	22	4	72	68	62%		No	25
EB		EB	48	18	11	79	68	37%		Yes	39
F	As Built	F	269	52	196	364	168	19%		No	245
FB		FB	229	55	151	299	148	24%		No	203
F	6X260°C	F	542	217	269	868	599	40%		Yes	448
FB		FB	320	113	158	520	362	35%		Yes	271
G	As Built	G	2000	0	2000	2000	0	0%		No	2000
GB		GB	1930	243	1159	2000	841	13%		No	2000
G	6X260°C	G	1511	628	591	2000	1409	42%		Yes	1533
GB		GB	1609	429	927	2000	1073	27%		Yes	1340
H	As Built	H	2000	0	2000	2000	0	0%		No	2000
HB		HB	1930	93	1731	2000	269	5%		No	1873
H	6X260°C	H	1930	242	1161	2000	839	13%		No	2000
HB		HB	1095	373	565	1665	1100	34%		No	925
I	As Built	I	1001	129	818	1179	361	13%		No	940
IB		IB	788	92	654	991	337	12%		No	745
I	6X260°C	I	668	169	431	1015	584	25%		Yes	594
IB		IB	565	264	280	1071	791	47%		Yes	460
High Speed FR4											
J	As Built	J	419	63	327	535	208	15%		No	389
JB		JB	291	50	218	383	165	17%		No	268
J	6X260°C	J	262	118	124	491	367	45%		Yes	215
JB		JB	277	86	152	462	310	31%		Yes	240
K	As Built	K	795	117	601	1094	493	15%		No	744
KB		KB	612	47	553	725	172	8%		No	591
K	6X260°C	K	364	81	229	544	315	22%		Yes	327
KB		KB	383	84	272	538	266	22%		Yes	345
L	As Built	L	2000	0	2000	2000	0	0%		No	2000
LB		LB	2000	0	2000	2000	0	0%		No	2000
L	6X260°C	L	1781	140	1529	1972	443	8%		No	1713
LB		LB	1649	253	1252	2000	748	15%		No	1532

Note: Data highlighted in red is based on delamination being present in the coupons, the data is considered suspect**.**

Ranking Material Performance

Table 11 shows a progressively ranking of each material's performance for the 3 material categories, from best to worse. The objective of the multiple tables is designed to show how material performance ranking is changed based on non-stressed and stressed test results, and is then confounded in situations where material damage is present.

The upper two tables represent the High Tg FR4 materials, this grouping is relatively straightforward because cohesive delamination was not found in any of the four constructions. The results of the non-stressed coupons (Before) is counterintuitive because in material "B" the higher resin content construction (69%) out-performed the lower resin content (58%). A reasonable argument could be made that based only on a low statistically sample size of 6 results, that this result is due to lower statistical confidence.

After the materials received 6X 260°C reflow cycles, the materials performances reverted back to their expected ranking. In the case of the High Tg FR4 materials the change in rankings are subtle, but confirms that differences in characteristics related to material, construction, variability in design, etc., should only be quantified in the stressed (reflowed) state.

The ranking for the Halogen Free materials grouping proved to be far more complex, due to the high fallout for cohesive damage experienced during the 6 reflow cycles. From the original 12 constructions only 3 materials designed with the 0.8mm/0.032" grid coupons were sufficiently robust enough to "survive" Pb free assembly, without damage.

When the non-stress results are ranked, each material and resin content fell perfectly in line, giving the impression that selecting the best material should be a formality. The results "after" still contain all of the results for both grid sizes, based on the possibility that the lab doing the testing did not know that material damage had occurred. The previously clear ranking before has now been replaced by a confusing order of material performances that would prove difficult for most statisticians and material experts to explain.

It is now necessary to introduce different screening techniques to enable a re-organization of rankings, bringing together via reliability performance with material integrity performance. As stated before high fallout was found on the 0.8mm/0.032" grid coupons, if the product design does not use this smaller grid size the material can be ranked by the 1mm/0.040" grid size. Screen 1 in table 6 removes all 0.8mm/0.032" grid results (12) and the 6 materials that exhibited cohesive damage on the 1mm/0.040" grid size. The results confirm that two candidates (H/HB and C/CB) achieved high to medium via reliability and proved to be thermally robust in assembly.

If the product design (based on device type) specifies that a 0.8mm/0.032" grid is required, screen 2 removes any materials that exhibited cohesive damage on the 0.8mm/0.032" and 1mm/0.040" grid sizes. The results of this process effectively reduced the ranking and possible selection options to one material (H/HB), from the original 6 candidates.

The High Speed FR4 materials grouping followed a similar trend to the Halogen Free materials. The "before" results are well organized and follow the performance expectations based on resin content. After assembly two material types (J and K) switched places, showing higher performance on the higher resin content constructions. Screen 1 removes all 0.8mm/0.032" grid results (8) and the 2 materials that exhibited cohesive damage on the 1mm/0.040" grid size, The ranking comes back into a reasonable alignment, with the exception of material "K". When the final screen is applied material "K" was eliminated because of the damage found in the 0.8mm/0.032" grid, this was considered grounds for rejection. Again, the final selection concludes with a single material type (L/LB), which demonstrated to be both highly reliable and thermally robust.

Completing an effective material ranking system is similar to peeling an onion, it is necessary to go through multiple layers of information to achieve an overall understanding of a material performance. An important element of this screening technique requires the decision maker to justify their criteria for acceptance and rejection of data. In the ranking demonstrated in this paper equal importance was placed on both via reliability and material integrity. If the product design uses larger grids sizes, has no high speed lines, a short life span, non-life critical, etc., for these cases the weighting for via reliability can take precedence over material integrity. Other important factors are material cost, material availability, electrical properties, contractual commitments to specific material vendors, etc., can all be factored into the screening process to select the best overall material.

Table 11

High Tg FR4

Before: Ranking of **Non-stressed** Coupons With Both Grids			After: Ranking of **Stressed** Coupons With Both Grids		
Coupon	Log N	Delam	Coupon	Log N	Delam
A	**646**	No	A	**453**	No
AB	**402**	No	AB	**337**	No
BB	**355**	No	B	**219**	No
B	**310**	No	BB	**155**	No

Halogen Free

Before: Ranking of **Non-stressed** Coupons With Both Grids			After: Ranking of **Stressed** Coupons With Both Grids			Screen 1: Ranking of **Stressed** 1mm/0.040" Coupons Only			Screen 2: Ranking of **Stressed** Coupons With Both Grids		
Coupon	Log N	Delam	Coupon	Log N	Delam	Coupon	Log N	Delam	Coupon	Log N	Delam
G	**2000**	No	H	**2000**	No	H	**2000**	No	H	**2000**	No
GB	**2000**	No	G	**1533**	Yes	HB	910	No	HB	**925**	No
H	**2000**	No	GB	**1340**	Yes	G	**869**	No	E	**25**	No
HB	**1873**	No	HB	**925**	No	C	**458**	No			
C	**852**	No	C	**498**	Yes	CB	**341**	No			
CB	**730**	No	F	**448**	Yes	E	**40**	No			
D	**482**	No	DB	**436**	Yes						
DB	**457**	No	CB	**433**	Yes						
F	**245**	No	FB	**271**	Yes						
FB	**203**	No	D	**265**	Yes						
E	**160**	No	EB	**39**	Yes						
EB	**104**	No	E	**25**	No						

High Speed FR4

Before: Ranking of **Non-stressed** Coupons With Both Grids			After: Ranking of **Stressed** Coupons With Both Grids			Screen 1: Ranking of **Stressed** 1mm/0.040" Coupons Only			Screen 2: Ranking of **Stressed** Coupons With Both Grids		
Coupon	Log N	Delam	Coupon	Log N	Delam	Coupon	Log N	Delam	Coupon	Log N	Delam
L	**2000**	No	L	**1713**	No	L	**1607**	No	L	**1713**	No
LB	**2000**	No	LB	**1532**	No	LB	**1383**	No	LB	**1532**	No
I	**940**	No	I	**594**	Yes	I	**505**	No			
IB	**745**	No	IB	**460**	Yes	KB	**339**	No			
K	**744**	No	KB	**345**	Yes	K	**285**	No			
KB	**591**	No	K	**327**	Yes	J	**173**	No			
J	**389**	No	JB	**240**	Yes						
JB	**268**	No	J	**215**	Yes						

Correlation of IST Results

A regression analysis was undertaken on various numbers of configurations. Comparing firstly the individual 0.8mm/0.032" and. 1mm/0.040" results, followed by the combined results. Graphs 10a compares the results from non-stressed and stressed conditions for all 0.8mm/0.032" grid coupons. The calculated R^2 was 0.8362, a respectable correlation. When the coupons that exhibited cohesive delamination and any results that exceeded 2000 cycles are removed, the calculated R^2 is improved to 0.8951 (see Graph 10b). The results of the 1mm/0.040" grid, shown in graphs 11a and 11b demonstrate a higher significance. The calculated R^2 for all material types, regardless of material integrity, was 0.8166. When the coupons that exhibited cohesive delamination and any results that exceeded 2000 cycles are removed, the calculated R^2 it improved to 0.929.

The combined results of both grid sizes, shown in graphs 12a and 12b confirm the calculated R^2 for all material types, regardless of material integrity, was 0.8936. When the coupons that exhibited cohesive delamination and any results that exceeded 2000 cycles are removed, the calculated R^2 it improved to 0.9343.

This data confirms that the presence of material damage and non-failed coupons was impacting to the ability to achieve a high level of statistically validity and ultimately correlation between data sets. The removal of confounding data improves the levels of correlation and confidence in the conclusions.

.

Graph 10a

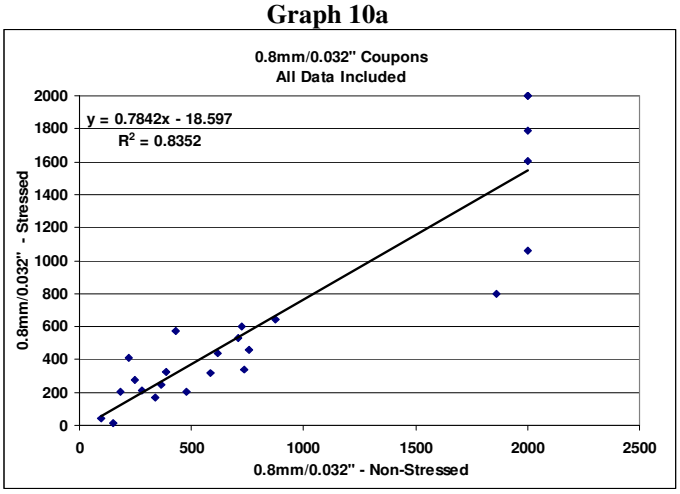

Graph 10b

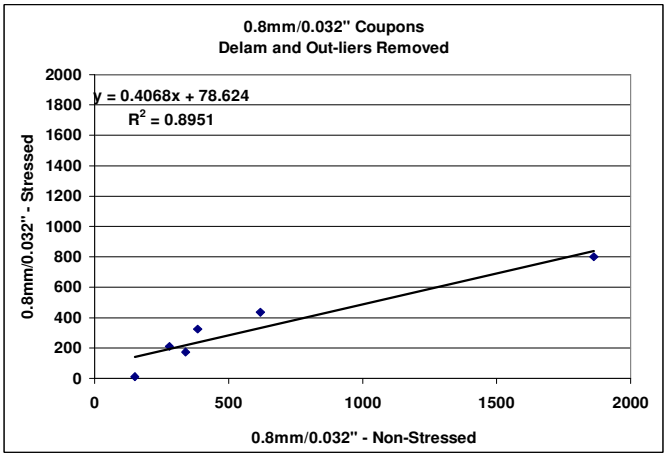

Graph 11a

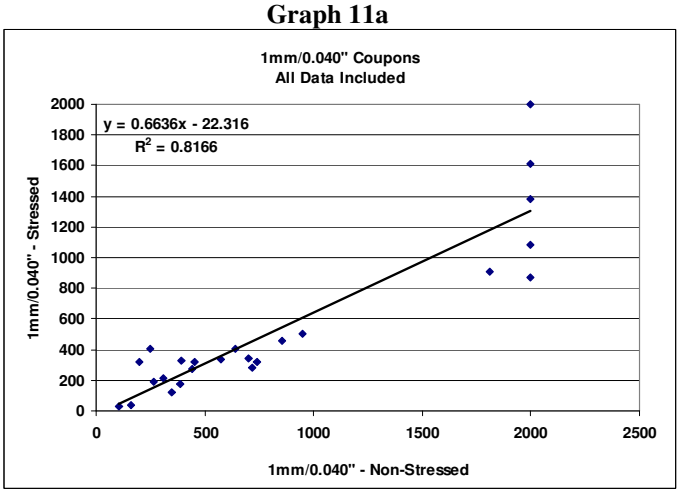

Graph 11b

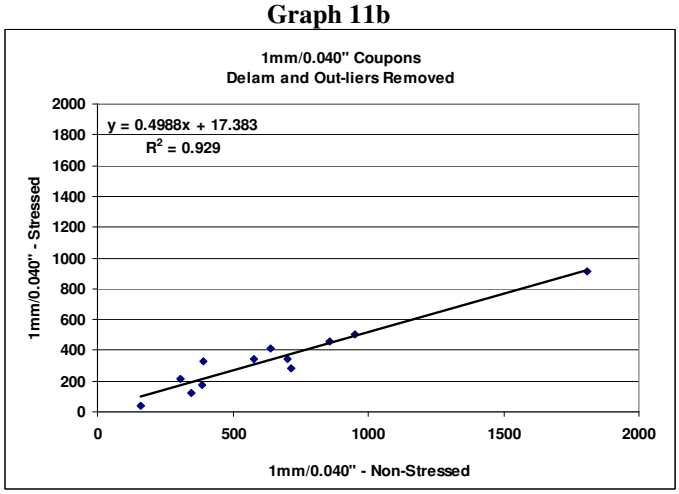

Graph 12a

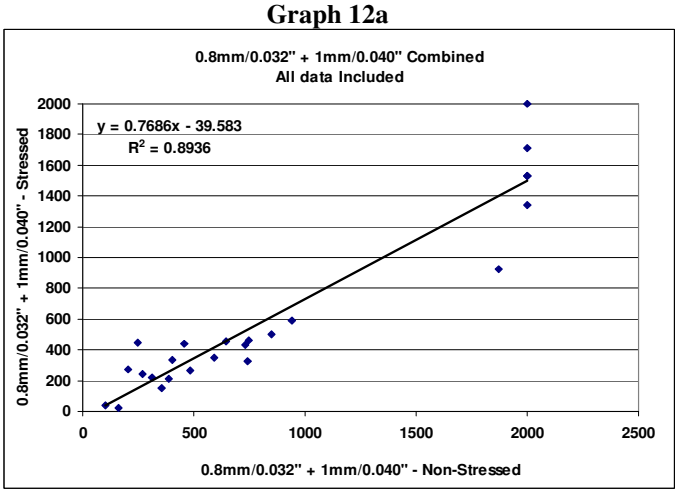

Graph 12b

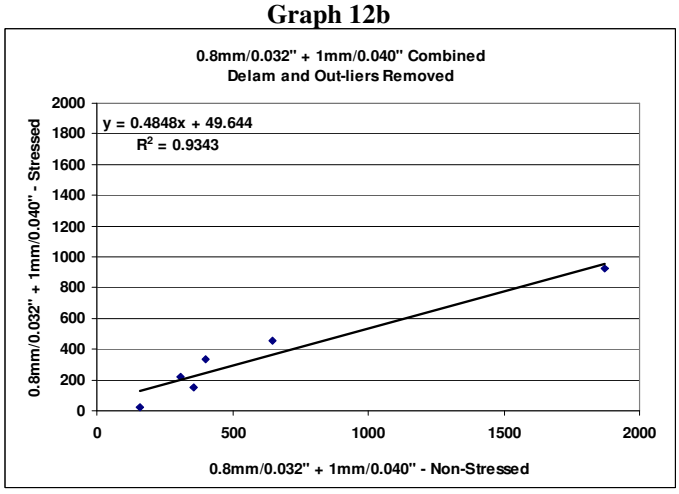

MATERIAL INTEGRITY STUDY CONCLUSIONS

- Fifteen of the 24 materials proved unsuitable after 6X 260°C Pb free assembly, specifically on the 0.8mm/.032" grid size. Eight materials proved unsuitable on the 1mm/.040" grid size.
- Certain "Pb free compatible" materials demonstrated delamination in the 2nd cycle of assembly, 10 materials delaminated in the 3rd cycle. Each preconditioning cycle produced increasing level material damage.
- Material damage through Pb free assembly was dominated by cohesive failure, primarily across the central zone of the construction.
- The nature of the cohesive damage is compromising the critical glass/resin interface. Laminate manufacturers must investigate this situation to understand root cause and introduce improvements.
- The MRT-5 IST test coupon design and DELAM testing protocol proved very effective at characterizing the presence, location and magnitude of material damage during and after Pb free assembly, achieving a 98% confidence when compared with microsection analysis.
- The electrical specification based on a minimum of 4% decrease in bulk capacitance demonstrated the ability to identify and confirm material damage.
- The result of conventional 6X solder float testing to 288°C did not achieve correlation with coupons that received 6X 260°C Pb free assembly.
- The material damage was not visible on the surface of the coupons, although major delamination was present throughout the construction. The majority of damage caused during assembly was focused toward the centre of the construction.

VIA RELIABILITY TESTING CONCLUSIONS

IST testing confirmed a wide range of via reliability performance levels amongst the 24 industry standard materials. Results ranged from immediate failures to no failures found at 2000 cycles. This is based on identical electrolytic copper plating conditions for all constructions.

Material damage has been demonstrated to be stress relieving in the areas of cohesive damage; copper cracks are effectively redistributed into different locations within the construction, for the same via structure. This conclusion does not automatically mean that cycles to failure will be greatly extended, but it should be understood that a critical area of the copper plated barrel will not be contributing to the crucial measurement of total damage accumulation.

There were 7 instances (out of 24) where PTH via reliability performances were increased following exposure to 6X 260°C reflow cycles, compared to non-stressed results. The combined effects of stress redistribution and stress relieving across the central zone of the copper plated barrel are considered to be the primary explanation.

Grid sizes of 0.8mm/0.032" are 2X more susceptible to cohesive material damage during multiple Pb-free reflow cycles compared to 1mm/0.040". Fifteen out of 24 materials exhibited multiple levels of cohesive delamination in 0.8mm/0.032" coupons compared to "only" 8 materials in 1mm/0.040" coupons. The poor result associated to the 24 industry standard materials is considered a very disappointing overall performance, indicating that the laminate industry has not achieved the desired advancements in the area of material integrity.

Any future PWB PTH thermal cycling reliability studies that combine grid sizes of 1mm/0.040 or smaller, and will apply multiple exposures to Pb-free reflow assembly must anticipate the requirement to quantify the presence of material damage in their testing protocols.

Material suitability for Pb-free assembly reflow cannot be determined by visual inspection alone. Using methodologies like DELAM testing is a complementary strategy to finding material damage in test vehicles. Combining the two methods will enable the ability to quantify the presence, location and magnitude of cohesive (or adhesive) damage within a PWB construction.

The majority of cohesive damage was found in the same location of the construction as where copper fatigue cracks were expected to initiate and propagate.

Failure analysis confirmed that the test boards were well constructed, with high quality copper plating. The common failure mode was copper fatigue of the plated barrel, the fatigue cracks were consistent with a wear out failure mode.

The IST damage accumulation graphs confirmed the majority of coupons failed due to an expected accelerating type of damage profile. These two combined results confirm high quality copper plating, on the part of the PWB manufacturer.

In the ranking system demonstrated in this paper equal importance was placed on both the performance of via reliability and material integrity. Quantifying the overall PTH via reliability performance proved difficult when attempting to make a material ranking, due to the confounded effects of cohesive material damage.

ACKNOWLEDGEMENTS

The author wants to thank the many unnamed people behind the scenes that contributed greatly to this work and to specifically acknowledge Kim Morton of Viasystems and support staff at Viasystems China for their massive committment to construct the 24 different material builds. In addition their work in support of failure analysis effort. John Wilson of IBM, the project leader, and Brian Smith, the HDP Users Group project facilitator also played a major role in making this project a success. Thilo Sack of Celestica, for coordinating the reflow assembly. David Birch for the extensive effort to collate, graph and the mammoth effort to report the results of testing, in addition to the data collection and imaging created during the failure analysis phase. Jason Furlong for his tremendous knowledge and contribution to completing the statistical analysis. Joe Smetana of Alcatel Lucent for his personal support to collate the diversity of information with wisdom and knowledge throughout this extensive study.

REFERENCES

[1] Smetana, J., Birch, B., Sack, T., Morton, K., Yu, M., Katzko, C., Helminen, E., "Reliability Testing of Pb-Free PWB Plated Through Holes in Air-to-Air Thermal Cycling and Interconnect Stress Testing", IPC/APEX, Las Vegas NV, 2011.

[2] Birch, B., Furlong, J., "Materials Testing of PWB Substrates to Establish Variability of Construction, Estimate Thickness and Determine Survivability Through Lead Free Assembly", IPC/APEX, Las Vegas NV, 2011.

[3] Smetana, J., Birch, B., Rothschild, W., "A Standard Multilayer Printed Wiring Board for Material Reliability Evaluations", IPC/APEX, Las Vegas NV, 2011.

[4] Birch, B., Furlong, J., "Materials Testing of PWB Substrates to Determine Survivability Through Lead Free Assembly", SMTAI, Dallas/Fort Worth TX, 2013

[5] Xu C., Kopf R., Smetana J., Fleming D., "Moisture Sensitivity and Its Effect on Delamination". IPC/APEX, Las Vegas NV, 2011.